

---

# Methods<sup>1</sup>

---

## Expedition 302 Scientists<sup>2</sup>

### Chapter contents

<b>Introduction</b> .....	<b>1</b>
<b>Lithostratigraphy</b> .....	<b>5</b>
<b>Micropaleontology</b> .....	<b>7</b>
<b>Stratigraphic correlation</b> .....	<b>10</b>
<b>Petrophysics</b> .....	<b>13</b>
<b>Geochemistry</b> .....	<b>19</b>
<b>Microbiology</b> .....	<b>23</b>
<b>Paleomagnetism</b> .....	<b>25</b>
<b>References</b> .....	<b>25</b>
<b>Figures</b> .....	<b>30</b>
<b>Tables</b> .....	<b>40</b>

### Introduction

Information assembled in this chapter will help the reader understand the basis for the preliminary conclusions of the Expedition 302 Scientists and will also enable the interested investigator to select samples for further analyses. This information concerns offshore and onshore operations and analyses described in the “**Sites M0001–M0004**” chapter. Methods used by various investigators for shore-based analyses of Expedition 302 samples will be described in the individual contributions published in the Expedition Research Results and in various professional journals.

### Authorship of site chapter

The separate sections of the site chapter were written by the following authors, listed in alphabetical order:

Expedition summary and principal results: Expedition 302 Scientists

Background and objectives: Backman, Moran

Operations (Methods): Graham, Röhl, Skinner, Wallrabe-Adams  
Operations: Skinner

Sedimentology: Clemens, Matthiessen, St. John, Stein, Suzuki, Watanabe (and observer Krylov)

Biostratigraphy: Brinkhuis, Cronin, Eynaud, Jordan, Kaminski, Koç, Matthiessen, Moore, Onodera, Rio, Suto, Takahashi

Timescale and sedimentation rates: Backman, Moore, Pälike

Stratigraphic correlation: Pälike, O’Regan

Petrophysics: Jakobsson, Moran, O’Regan, Pälike, Rea, Sakamoto

Geochemistry: Dickens, Martinez, Stein, Yamamoto

Microbiology: Smith

Paleomagnetism: Gattacceca, King

Geophysics: Jakobsson (and non-expedition scientists Coakley, Edwards, Flodén, Jokat, Kristoffersen)

### Offshore and onshore science activities

Expedition 302, Arctic Coring Expedition (ACEX), science activities were partially conducted offshore during the field expedition aboard the *Oden* and *Vidar Viking* and completed onshore at the Integrated Ocean Drilling Program (IODP) Bremen Core Repository (BCR) after the expedition. A subset of the expedition scientists participated in the offshore phase of Expedition 302, and all expedition scientists participated onshore.

<sup>1</sup>Expedition 302 Scientists, 2006. Methods. In Backman, J., Moran, K., McInroy, D.B., Mayer, L.A., and the Expedition 302 Scientists. *Proc. IODP, 302*: Edinburgh (Integrated Ocean Drilling Program Management International, Inc.). doi:10.2204/iodp.proc.302.103.2006

<sup>2</sup>[Expedition 302 Scientists’ addresses.](#)



This chapter is organized by discipline, and each section describes the methods and standard procedures used in both the offshore and onshore phases.

Cores were collected offshore in lengths of up to 5 m, cut into 1.5 m lengths, nondestructively tested using the multisensor core logger (MSCL), stored in a refrigerated container, and then transported to BCR after the offshore phase ended. Core catchers from each core were analyzed offshore for biostratigraphy, visual core description, moisture and density (MAD), and chemistry. A limited suite of whole-round samples was taken from cores collected for offshore analyses, pore water sampling, and microbiology. MAD samples were taken and analyzed offshore. Onshore, at BCR, cores underwent the complete IODP suite of analyses and sampling by the expedition scientists. Methods describe offshore and onshore activities, including biostratigraphy, lithostratigraphy, timescale and sedimentation rates, stratigraphic correlation, petrophysics, chemistry, and microbiology.

## Coring methods

### Drilling and coring tools

A number of different coring tools were mobilized for Expedition 302, including a complete back-up system of wireline coring tools in case the requested tools did not perform as anticipated or losses were greater than the three complete sets of new equipment carried. In the event that only the new coring tools were used, the level of new system spares carried was sufficient for all of the work conducted.

All drilling operations were contracted to Seacore Ltd. of Gweek (Cornwall, U.K.), who constructed, installed, and operated an R100 rig designed for cold-weather operations. The rig was installed on the Expedition 302 drillship (*Vidar Viking*), a modified ice-breaker ICE-10 class ship with dynamic positioning. During drilling, officers on board positioned the vessel manually by joystick control. A 2 m diameter moonpool was installed with an underhull steel skirt that protected the drill string from damage or severing by ice.

### Drill string

A Deep Sea Drilling Project (DSDP)/Ocean Drilling Program (ODP) 5 inch drill string with 5½ inch full hole connections and a 4⅞ inch inner diameter (ID) was used. It was downgraded to grade 2 but was acceptable for Expedition 302 requirements. All pipes were prepared at Texas A&M University (TAMU) or Houston (Texas, USA) and shipped to the United Kingdom in pipe bins specially made in Houston for the British Geological Survey (BGS). These pipe bins were also used for pipe storage on the drillship dur-

ing operations. BGS acquired 2.5, 3.5, and 5 m “pup” joints machined from solid bar to allow for “spacing out” and setting up the top drive. All of the new joints were of certified American Petroleum Institute (API) materials, manufacture, and threads.

### Drill collars

Drill collars were provided by the drilling contractor, Seacore Ltd. All were Certified API materials and threads (7 inch outer diameter (OD) [178 mm], 4 inch ID [101 mm], and 5 m long) and were new for the project.

### Coring tools

The coring tools used belonged to the new BGS Marine Wireline Corebarrel System (BGS-MWCBS). This system uses a common outer core barrel assembly to house wireline-retrievable tools for piston coring, extended coring, push coring, and nonrotating hard rock coring. A separate inner tube configuration allows push sampling or probe (e.g., temperature) insertion at the base of the hole, and an insert full-face drill bit can be added to allow open-hole wash drilling in selected borehole intervals. A sliding hammer was also fabricated on board, and a modified version of the hammer will be added to the suite of tools carried on any future operations with the BGS-MWCBS.

### Outer core barrel assembly

The outer core barrel assembly is a 7 inch (178 mm) OD steel tube 7 m long with a section at the bottom that accepts a drill bit, a honed ID central section to allow a sealed bore for piston coring, and a set of top sections to allow for inner barrel landing and latching. All materials, manufacture, and threads on the core barrel were to API standard with 5½ inch full hole threads to match the bottom-hole assembly (BHA) except for two subs, where the pin section had a modified length to allow for inner rings. The box thread on the head section of the outer core barrel is directly compatible with the drill collar threads used for the BHA.

The drill bits used with the system were 9½ inch OD (242 mm) with a clear 98 mm ID through which tools or seat core bits were passed. Three types of bits were aboard the ship: natural diamond, polycrystalline diamond, and six-cone roller. Only the six-cone roller bit was used.

### Piston corer

The piston corer (PC) is a modified version of the ODP advanced piston corer (APC) system which, with the exception of orientation, was made to the same specification with the same materials. The main difference is that the PC is 5 m in length so

that the tool could be used with smaller drill rigs. Various flapper, dog, and basket catchers were carried, and standard ODP core liner was used.

### **Extended corer**

The extended corer is similar to the ODP extended core barrel (XCB) in that it is designed to obtain core in “difficult formations.” It is a rotating core barrel that extends some 100 mm ahead of the main drill bit and collects core from there. However, if the material becomes too hard for core collection, then a spring assembly allows the small XCB bit to retract into the face of the main drill bit that then assists with the coring as well as the hole cutting. Replacing the cutting end enables the best core recovery, and a variety of bits, cutting shoes, and catchers are available for the extended corer. The BGS extended corer also uses standard ODP core liner.

### **Latch-in indicator and nonreturn valve systems**

Incorporated into the landing and latching assemblies of all but the piston corer inner assemblies are two features that allow indication of latch-in and nonreturn of fluids up the drill pipe should unexpected pressures be encountered in the formation.

### **Wireline retrieval system**

Wireline retrieval is by means of a standard Boart Longyear PQ overshot. An overshot fishing tool and release sleeves compatible with the tool but modified by BGS for deepwater work were also available but were not used. All inner core barrels latch onto the overshot retrieval tool using a Boart Longyear Spear Point Assembly. Bridon Fibres Ltd. provided the special wireline wire, selected on the recommendation of Weatherford, who also supplied the termination. This wire allowed a packer to be deployed around it to seal the borehole for piston coring.

### **Core handling and curation**

Once the coring tool arrived on deck, the plastic-lined core was removed from the core barrel and each core was cut into 1.5 m sections and labeled. Consistent with IODP policy, all cores were named and labeled with the appropriate expedition number, site number, hole letter, core number, core type (Table T1), section number, and an indication of whether a split-core half was working or archive. Samples and data labels also included the sample interval.

Cores taken from a hole were numbered serially from the top of the hole downward. When full recovery

was obtained, core sections were numbered 1 through 3 or 4, beginning at the top of the core. The core catcher sample was extruded into a short piece of split plastic liner and treated as a separate section below the last core section.

When sediment recovery was <100%, the recovered sediment was measured from the top of the cored interval and then each of the sections were numbered serially, starting with section 1 at the top. Sections were cut starting at the top of the recovered sediment so that the lowest section was in many cases shorter than the nominal 1.5 m section length.

Core sections were labeled at each end, and the working (double line) and archive (single line) side of the liners were engraved with the standard IODP identifier, “Expedition-Site-Hole-Core-Core type-Section” (e.g., 302-M0001A-1H-1, W) along with an “up” arrow. This ensured that each section could be permanently and uniquely identified. Blue end-caps (top of section) were marked with the core, core type, and section number (Fig. F1).

At section breaks, the liner was cut with a liner pipe-cutting tool and the sediment was separated with a wire saw or spatula, depending on the level of sediment induration. Core sections were then moved into the curation container and capped. Caps were temporarily fastened until whole cores were taken for geochemistry and microbiology. Blue end-caps were placed at the top of each section, with clear end-caps at the bottom.

Whole-round samples were taken after MSCL core logging (see “[Petrophysics](#)”), provided that the logging was completed within 40 min of recovery. Whole-round samples were taken on a selected basis at an interval of approximately one every third core. Yellow end-caps were placed at the end of any section from which a whole-round sample was taken.

Core sections were not split offshore, and onboard sampling was limited to whole-round and core catcher samples. Although most sampling was conducted during the onshore science party at BCR, shipboard scientists (microbiologist and geochemists) collected samples offshore because of the ephemeral nature of these properties.

All full core sections, core catcher samples, and some pore water aliquots were stored in the temperature-controlled container aboard the drillship. Pore water subsamples that required freezing were sent and stored aboard the *Oden* at  $-20^{\circ}\text{C}$  (see “[Geochemistry](#)”). Microbiology samples were further treated, subsampled, and stored for different types of analyses (see “[Microbiology](#)”).

## Data handling, database structure, and access

Data management during offshore and onshore phases of Expedition 302 had two overlapping stages. The first stage was the capture of metadata and data during the expedition (offshore and onshore). Central to this was the ACEX-Offshore Drilling Information System (OffshoreDIS), which stored drilling information, core curation information, and primary measurement data. The second stage was the longer-term postexpedition archiving of Expedition 302 data sets, core material, and samples. This function was performed by the World Data Center for Marine Environmental Sciences (WDC-MARE) and BCR.

OffshoreDIS is a flexible and scalable drilling information system, originally developed for the International Continental Drilling Program (ICDP). The underlying data model for OffshoreDIS is compatible with Janus, BCR, PANGAEA, and LacCore in Minneapolis (Minnesota, USA). For the specific expedition platform configuration and offshore and onshore workflow requirements of Expedition 302, the OffshoreDIS data model, data pumps, and user interfaces were adapted to form ACEX-OffshoreDIS. This was the first implementation of OffshoreDIS, so it was very much a test of the system. Consequently, improvements and enhancements to the underlying database tables and user interfaces were made as a result of experience gained both during the expedition and postexpedition, which will serve future IODP mission-specific platforms (MSPs) and ICDP expeditions.

Offshore, the system captured basic information related to core and sample curation, core photographs, section and sample label printing, and daily drilling logs. In addition, the database also stored primary data measurements. These included

- Geophysical downhole logging data (from the European Petrophysics Consortium [EPC] management office, University of Leicester);
- MSCL data;
- Visual core descriptions; and
- Gas, chemical, and temperature measurements.

In practice, it was not possible to capture some data sets during the offshore phase because the data model was incompatible with the actual data captured (e.g., MSCL calibration data). Also, scientists produced a variety of spreadsheet files and text documents containing data, descriptions, and interpretations in many different formats. Therefore, in addition to ACEX-OffshoreDIS, all data files were stored in a structured file system on a shared hard drive.

For the onshore phase, the system was expanded to manage additional data types, and deficiencies in

the original implementation were corrected. In addition, a visual core description tool, a Web interface, and a file management system were developed.

Expedition 302 data were then transferred to the information system of WDC-MARE during the second phase. WDC-MARE was founded in 2000 and is a member of the International Council of Scientific Unions World Data Center system. PANGAEA is the geoscience information system used by WDC-MARE. It has a flexible data model that reflects the information processing steps in Earth science fields and can handle any related analytical data (Diepenbroek et al., 1999, 2002). It is used for processing, long-term storage, and publication of georeferenced data related to Earth sciences. Essential services supplied by WDC-MARE/PANGAEA are project data management and distribution of visualization and analysis software. Data management functions include quality checking, data publication, and metadata dissemination following international standards.

Data captured by the ACEX-OffshoreDIS were transferred to this long-term archive following initial validation procedures as soon as they became available; data transfer was completed by the time of publication of this IODP *Proceedings* volume. Until the end of the moratorium period, the data were not public and access was restricted to the expedition scientists. However, following the moratorium, the data were published on the Internet ([www.wdc-mare.org](http://www.wdc-mare.org)) and WDC-MARE will continue to acquire, archive, and publish new results derived from Expedition 302 samples and data sets. OffshoreDIS was not able to produce standard barrel sheets for this volume. Visual core descriptions (VCDs) were manually reentered into AppleCORE for this purpose at the University of Rhode Island (USA). Future MSP expedition managers should consider VCD presentation during project planning stages.

## Hardware installation

OffshoreDIS was implemented in SQLServer2000 with Microsoft-based client PCs connected to the system through a Microsoft Access-like user interface. For the offshore phase of the expedition, OffshoreDIS was installed on servers on both the *Vidar Viking* and the *Oden*. The system was configured to provide merge replication with the primary server on the *Vidar Viking*. This allowed the parties on both ships to operate independently in case of breaks in intership communications. In practice, the communications worked very well and the second server on the *Oden* was used as a hotstandby and data backup system.



## Core, section, and sample curation using ACEX-OffshoreDIS

IODP procedures and naming conventions were followed during Expedition 302 in core, section, and sample handling (see “[Core handling and curation](#)”). OffshoreDIS handled the curation of data and printed the appropriate labels also to IODP standards.

Curation data comprise the following:

- Expedition information;
- Site information (latitude, longitude, water depth, start date, and end date);
- Hole information (hole naming by a letter, latitude, longitude, water depth, start date, and end date);
- Core data (core number, core type, top depth, bottom depth, number of sections, core catcher availability, curator, core on deck, date and time, and additional remarks);
- Section data (section number, section length, curated length, curated top depth of section, section length, and curated length);
- Sample information (repository, request, request part, code observer, expedition, site, hole, core, section, half, sample top, sample bottom, and sample volume);
- Calculated core recovery percentage on the basis of the drilled or cored length and the curated recovery; and
- Calculated section recovery on the basis of the section length and the curated length. No correction was made in cases where recovery exceeded 100%. Top and bottom depth of the section (meters below seafloor [mbsf]) was calculated on the basis of the core-top depth. Curation of subsections was also possible but was not used during Expedition 302.

Section and sample label formats follow standard ODP/IODP conventions. They include the barcodes of the section/sample code and the complete section/sample code (Expedition-Site-Hole-Core-Core type-Section-Half-Interval and sample request code). This standardization guarantees data exchange among the repositories and enables information flow between the implementing organizations.

## Lithostratigraphy

### Visual core descriptions

Expedition 302 sedimentologists were responsible for visual core descriptions and smear slide analysis of cored sediment and rock. Lithology of recovered

material is recorded on the barrel sheets (found in “Core Descriptions”) using symbols to represent up to three components in the Graphic Lithology column (Fig. F2). Where an interval of sediment is a mixture of lithologic components, the constituent categories are separated by a solid vertical line, with each category represented by its own symbol. In contrast, constituent categories separated by a dashed vertical line indicate intervals of thinly interbedded sediments comprising two or more lithologies of different compositions. Constituents accounting for <10% of the sediment in a given lithology are not shown in the Graphic Lithology column but are listed in the Lithologic Description section of the core description form. Because of the limited scale of the core summaries, the Graphic Lithology column usually shows only the composition of layers or intervals exceeding 20 cm in thickness.

The Structure column indicates the presence of primary sedimentary structures, soft-sediment modification features, structural features, and diagenetic features observed visually (Fig. F3). The following definitions were adopted from Blatt et al. (1980, p. 128):

- Thick bedding/color banding = beds/bands > 30 cm thick.
- Medium bedding/color banding = beds/bands 10–30 cm thick.
- Thin bedding/color banding = beds/bands < 10 cm thick.

The following scale is used to describe bioturbation as measured by the percentage of burrow features:

- Slightly bioturbated = 1%–30% bioturbation.
- Moderately bioturbated = 30%–60% bioturbation.
- Heavily bioturbated = 60%–90% bioturbation.

Total mixing of sediment by bioturbating organisms produces homogeneous sediment with an appearance similar to nonbioturbated sediments that result from the deposition of material of homogeneous color and grain size. Therefore, a bioturbation scale cannot be applied to homogeneous sediment with confidence.

Deformation and disturbances of sediment that clearly resulted from the coring process are illustrated in the Drilling Disturbances column of the barrel sheets (see “Core Descriptions”). The degree of drilling disturbance is described for soft and firm sediments using the categories listed below (blank regions indicate the absence of drilling disturbance):

- Slightly disturbed = bedding contacts that are slightly bent or drilling biscuits that are unrotated and in stratigraphic order.

- Moderately disturbed = bedding contacts that are extremely bowed or sediment biscuits that are rotated but likely still in stratigraphic order.
- Very disturbed = bedding that is completely disturbed or sediment biscuits that are likely rotated and no longer in stratigraphic order.
- Drilling slurry or flow-in = intervals that are water-saturated or have otherwise lost all aspects of original bedding resulting from flow-in or the presence of drilling slurry.

The degree of fracturing in indurated sediments is described in the Drilling Disturbance column using the following categories:

- Slightly fractured = core pieces that are in place and contain little drilling slurry or breccia.
- Moderately fragmented = core pieces that are in place or partly displaced, but the original orientation is preserved or recognizable (drilling slurry may surround fragments).
- Highly fragmented = pieces that are from the cored interval and probably in the correct stratigraphic sequence (although they may not represent the entire section), but the original orientation is completely lost.
- Drilling breccia = core pieces that are no longer in their original orientation or stratigraphic position and may have been mixed with drilling slurry.

The hue and chroma attributes of color are recorded in the Color column of the barrel sheet and were determined using Munsell Soil Color Charts (1971).

Figures summarizing key data from smear slides and XRD analyses appear in the “[Sites M0001–M0004](#)” chapter.

The lithologic description that appears in the Description column of each barrel sheet lists all the major and minor sediment lithologies observed in the core, as well as a more detailed description of these sediments including features such as color, composition (determined from the analysis of smear slides), or other notable characteristics. Descriptions and locations of thin, interbedded, or minor lithologies or thin color banding that could not be depicted in the Graphic Lithology column are included in the text. Terms to describe sediment induration (e.g., firm) follow those used during ODP Leg 105 (Shipboard Scientific Party, 1987).

## X-ray diffraction

### Equipment parameter

X-ray diffraction (XRD) measurements were performed at the Crystallography Department of Geosciences, University of Bremen, on a Philips X’Pert

Pro X-ray diffractometer equipped with a Cu tube ( $K_{\alpha}$ ,  $\lambda$  1.541), a fixed divergence slit ( $1/4^{\circ}2\theta$ ), a 15-sample changer, a secondary monochromator, and the X’Celerator detector system. Measurements were made from  $3^{\circ}$  to  $85^{\circ}2\theta$  with a calculated step size of  $0.016^{\circ}2\theta$ . The calculated time per step was 100 s. Peak identification was done graphically through the MacIntosh program MacDiff (version 4.5) (available at [servermac.geologie.uni-frankfurt.de/Staff/Homepages/Petschick/RainerE.html](http://servermac.geologie.uni-frankfurt.de/Staff/Homepages/Petschick/RainerE.html)) (Petschick et al., 1996).

## Mineral identification

Integrated intensities for the investigated mineral peaks were calculated by MacDiff. Based on this intensity, ratios were calculated. To provide an easy comparison to published data on surface samples of the potential source regions (Andersen et al., 1996; Vogt, 1997; Vogt et al., 2001), the fixed divergence was changed to automatic divergence using an algorithm integrated in MacDiff.

## Sediment classification

Expedition 302 sediment classification is based primarily on visual core descriptions and smear slide analyses. A modified version of the sediment classification format established during ODP Leg 151 (Shipboard Scientific Party, 1995) is used here to allow for easier comparison of the lithostratigraphy of cores retrieved during both cruises. As during Leg 151, the principal lithologic name (e.g., diatom ooze, silty clay) is based on the major (>50%) sediment component. Secondary components, composing 25% to 50% of the sediment, are included as major modifiers preceding the principal name (e.g., diatom ooze, silty clay). Minor constituents, composing 10% to 25% of the sediment, are included using the term “-bearing” (e.g., mud-bearing diatom ooze). The sediment modifiers are ordered so that minor modifier(s) precedes major modifier(s). Specific nomenclature for the two compositional groups, appropriate for sediments recovered during this expedition, is given below.

### Siliciclastic sediments

The siliciclastic category includes sediments having >50% siliciclastic sediments. These sediments are classified on the basis of grain size (Fig. F4). Siliciclastic sediment having >75% of a single component are given the name of that major component. For example, siliciclastic sediment containing 80% clay and 20% silt would be classified simply as “clay.” When siliciclastic sediment consists of a two-component mixture, the major component is preceded by a

modifier describing the secondary grain size. For example, siliciclastic sediment containing 70% clay and 30% silt would be classified as “silty clay.” In situations where the siliciclastic sediment contains a mixture of sand, silt, and clay and the least abundant of these components comprises 10% of the sediment, the term “mud” is given as the major component and is modified by the name given to the most abundant grain size. For example, a mixture of 10% sand, 60% silt, and 30% clay would be classified as “silty mud.”

### Biogenic sediments

The biogenic category includes fine-grained sediments containing >50% biogenic sediments. Designation as siliceous or carbonate depends upon the relative abundance of these two biogenic categories (Fig. F5). When the biogenic component is >90%, the sediment is classified as ooze. When biogenic sediments are mixed with 10% to 25% siliciclastic components, the siliciclastic component name followed by the word “-bearing” is used as a major modifier. For example, if the sediment contains 80% biogenic silica of mixed types (e.g., diatoms, ebridians, and silicoflagellates) and 20% siliciclastic clay, it would be classified as “clay-bearing biosiliceous ooze.” When the siliciclastic component is a mixture of sand, silt, and clay, the modifier “mud-bearing” is used (e.g., mud-bearing siliceous ooze).

## Micropaleontology

### Calcareous nannofossils

The zonal scheme of Martini (1971) was used for Cenozoic calcareous nannofossil biostratigraphy. This zonation represents a general framework for biostratigraphic classification of calcareous nannofossil assemblages. Many additional nannofossil biohorizons are also used for dating and correlation. Nannofossil taxonomy follows that of Perch-Nielsen (1985a).

Calcareous nannofossils were examined on smear slides using standard light microscope techniques under cross-polarized and transmitted light at 1000× magnification. The following abbreviations were used to describe nannofossil preservation:

- G = good (little or no evidence of dissolution and/or recrystallization; diagnostic characters fully preserved).
- M = moderate (dissolution and/or secondary overgrowth; partially altered primary morphological characteristics; most specimens were identifiable to the species level).

- P = poor (severe dissolution, fragmentation, and/or overgrowth; primary morphological characteristics largely destroyed; specimens often could not be identified at the species and/or generic level).

Five calcareous nannofossil abundance levels are recorded as follows:

- A = abundant (>10 specimens observed/field of view [FOV]).
- C = common (5–10 specimens observed/FOV).
- S = scarce (1–5 specimens observed/FOV).
- R = rare (<1 specimen observed/FOV).
- B = barren.

### Diatoms

The Neogene Nordic Seas diatom zonation of Koç and Scherer (1996), the North Pacific diatom zonation of Akiba (1986), and the Neogene North Pacific diatom (NPD) zone code system of Yanagisawa and Akiba (1998) are used for the Neogene intervals. The Oligocene and Eocene zonation is modified from the Norwegian Sea diatom zonation of Schrader and Fenner (1976), Dzinoridze et al. (1978), Fenner (1985), and Scherer and Koç (1996). Absolute ages for diatom biostratigraphic horizons were updated from the Cande and Kent (1995) geomagnetic polarity timescale (GPTS).

Most slides were prepared as smear slides. However, strewn slides were prepared from the core catcher samples using the method of Akiba (1986) by placing a small amount of material in a snap-cap vial and removing part of the upper suspension with a pipette. The sample (~1 g) was placed in a 250 mL beaker, heated at 100°C for 1–2 h, and broken into pieces, after which 100 mL of boiling distilled water was added. After the distilled sample soaked for 6 h, the supernatant fluid was skimmed. Additional distilled water was then added to obtain a solution of suitable density. The solution was left for 30 s to let grains denser than diatoms, such as grains of quartz, settle to the bottom of the beaker. Strewn slides were prepared by spreading the pipette suspension on a coverslip (22 mm × 30 mm), drying on a hot plate (50–60°C), and mounting in Pleurax.

Slides were examined under an Olympus BX41 microscope at 400× magnification, with identifications checked at 1000× magnification. On all slides, the abundance of total diatoms and other biosiliceous components, together with assemblage composition, were recorded. In core catcher samples, whenever possible, 200 specimens (other than *Chaetoceros* resting spores) were counted. After counting, the slides were scanned to record the presence of other species missed in the original tally. Between 100 and 1000

valves were observed for samples containing sufficient diatom remains. When fewer than 200 diatom valves were encountered on a slide, all taxa were enumerated in a single count.

Except for the core catcher samples, assessment of total diatom abundance was qualitative. Diatoms were recorded as follows:

- A = abundant ( $\geq 6$  specimens/FOV).
- C = common (1–5 specimens/FOV).
- F = few (1–4 specimens/5 FOV).
- R = rare (1–10 specimens/horizontal traverse).

Diatom preservation categories reported in the range charts are described according to Koç and Scherer (1996) as follows:

- G = good (finely silicified and robust forms present; no significant alternation of the frustules other than moderate fragmentation).
- M = moderate (concentration of more heavily silicified forms and/or a high degree of fragmentation of finely silicified forms).
- P = poor (finely silicified forms virtually absent; heavily silicified forms fragmented and/or corroded).

### Silicoflagellates

Prior to Expedition 302, silicoflagellates had not been observed in any sediment from the Lomonosov Ridge. Previous silicoflagellate studies from neighboring regions, however, including the Alpha Ridge in the Arctic Ocean, were used for reference. Based on the sediments recovered during Leg 151 from the Fram Strait and the Norwegian-Greenland Sea, a biostratigraphic zonal scheme has been established for the early Eocene through the Quaternary (Locker, 1996). Amigo (1999) worked on ODP Leg 162 materials from the Iceland and Rockall plateaus, and proposed new Miocene silicoflagellate zones. Perch-Nielsen (1985b) compiled comprehensive references on silicoflagellate biostratigraphy from the World Ocean. Silicoflagellates and ebridians were reported from the Alpha Ridge in Core FL-422 (Bukry, 1984; Ling, 1985; Dell'Agnese and Clark, 1994). Estimated ages were all adjusted to the GPTS for Expedition 302.

Core catcher samples were disaggregated and decalcified by gentle boiling in a solution of 10%  $\text{H}_2\text{O}_2$  and 10% HCl for ~2 h. A solution of Calgon was added to the sample solution and thoroughly stirred to further disaggregate the sediments and raise the pH level. Distilled water was repeatedly added to neutralize the sample solution before sieving through a 45  $\mu\text{m}$  stainless steel screen. Smear slides of both the coarse fraction ( $>45 \mu\text{m}$ ) and the fine fraction ( $<45 \mu\text{m}$ ) were prepared by pipetting the sediments onto

glass slides. The water was allowed to evaporate, and a drop of xylene was added to purge the sediments of remaining water. Finally, Canada balsam was added to the slide, and a 22 mm  $\times$  50 mm coverslip was placed on top. The coarse fraction was primarily used for the study of silicoflagellates, although the fine fraction was also investigated to account for smaller-sized specimens ( $<45 \mu\text{m}$ ).

Total silicoflagellate and ebridian abundances were determined along eight traverses (perpendicular to the length of slide) at 400 $\times$  magnification, using the following convention:

- A = abundant ( $>50$  specimens).
- C = common (16–50 specimens).
- F = few (3–15 specimens).
- R = rare (2–3 specimens).
- T = trace (1 specimen).
- B = barren (none on a slide).

Preservation of silicoflagellates and ebridians was recorded as follows:

- G = good (majority of specimens complete, with minor dissolution and/or breakage).
- M = moderate (minor but common dissolution, with a small amount of specimen breakage).
- P = poor (strong dissolution and/or breakage; many specimens unidentifiable).

### Radiolarians

No radiolarian biostratigraphic zonation has been developed for the Arctic Ocean. However, a biostratigraphic scheme for the Norwegian Sea (e.g., ODP Leg 104, Goll and Bjørklund, 1989) extends back to near the base of the Miocene and contains 30 zones. It builds upon the study carried out during DSDP Leg 38 by Bjørklund (1976), which includes eight zones covering the Oligocene and Eocene. The radiolarian biostratigraphy used for Expedition 302 is based largely on these two radiolarian zonations. Other high-latitude zonations have been developed for the North Pacific Ocean (e.g., Kamikuri et al., 2004), but it is uncertain how applicable these zonations will be in the Arctic Ocean.

Samples were disaggregated by heating in a solution of 10%  $\text{H}_2\text{O}_2$ . Calcareous components were then dissolved by adding a 10% solution of HCl and sieved through a 45  $\mu\text{m}$  screen. When clumps of clay and radiolarians remained on the 45  $\mu\text{m}$  sieve after initial treatment, the coarse residue was returned to the beaker and soaked in a concentrated solution of NaOH for 1–5 min on a warm hotplate, immersed in an ultrasonic bath for no more than 5 s, and then resieved. A strewn slide was prepared by pipetting the microfossils onto a glass slide, allowing the water to evaporate, adding a drop or two of xylene and



some Canada balsam, and covering with a 22 mm × 40 mm glass coverslip. Alternatively, after drying, the glass coverslips were mounted using 8–12 drops of Norland optical adhesive 61.

Total radiolarian abundances were determined based on strewn slide evaluation at 100× magnification, using the following convention:

- A = abundant (>100 specimens/slide traverse).
- C = common (51–100 specimens/slide traverse).
- F = few (11–50 specimens/slide traverse).
- R = rare (1–10 specimens/slide traverse).
- T = trace (<1 specimen/slide traverse).
- B = barren (no radiolarians in sample).

Individual species abundances were recorded relative to the fraction of the total assemblages as follows:

- C = common (>2000 specimens/slide).
- F = few (200–2000 specimens/slide).
- R = rare (20–200 specimens/slide).
- VR = very rare (2–20 specimens/slide).
- + = trace (<2 specimens/slide).
- B = barren (no radiolarians in sample).

Preservation was recorded as follows:

- G = good (majority of specimens complete, with minor dissolution, recrystallization, and/or breakage).
- M = moderate (minor but common dissolution, with a small amount of specimen breakage).
- P = poor (strong dissolution, recrystallization, or breakage; many specimens unidentifiable).

## Foraminifers

Preparation methods used to obtain calcareous, agglutinated, and planktonic foraminifers include disaggregation and wet-sieving over a 63 μm sieve. The sieved residues were dried, and the foraminifers were separated from the sand fraction under a binocular microscope. Several methods were used to disaggregate the sediment sample, including boiling in hot Calgon solution. The volume of original core catcher sample was variable, but ~10–20 cm<sup>3</sup> was processed whenever possible. Abundances of the foraminifers per ~10–20 cm<sup>3</sup> sample are characterized as follows:

- A = abundant (>250 specimens).
- C = common (25–250 specimens).
- F = few (5–25 specimens).
- R = rare (1–5 specimens).
- B = barren (no foraminifers in sample).

## Calcareous benthic foraminifers

Calcareous benthic foraminifers have been studied from Legs 104 and 151 (Osterman and Qvale, 1989; Osterman and Spiegler, 1996; Osterman, 1996). Shallow-water, high-latitude benthic foraminifers from

Baffin Island, Greenland, and the North Sea have been extensively studied by Feyling-Hanssen and colleagues (e.g., Feyling-Hanssen et al., 1983; Feyling-Hanssen, 1990; Knudsen and Asbjørnsdottir, 1991). Quaternary calcareous foraminifers from central Arctic Ocean deep-sea cores have been studied by Scott et al. (1989), Ishman et al. (1996), and Polyak et al. (2004). Taken together, calcareous benthic foraminifers provide a means to correlate Pleistocene sediments from the central Arctic Ocean with those from adjacent regions.

## Agglutinated benthic foraminifers

No formal zonal scheme for agglutinated foraminifers yet exists for the Cenozoic of the central Arctic Ocean, as these microfossils have only been studied from comparatively short piston cores that recovered the last few glacial cycles (Evans and Kaminski, 1998). Fortunately, however, regional zonations have been set up for several areas along the circum-Arctic shelves, including the Cenozoic of the Beaufort Sea–MacKenzie Delta region (Schröder-Adams and McNeil, 1994; McNeil, 1997), the Paleogene of the Western Barents Sea (Nagy et al., 2000, 2004), and the Paleogene of the western Siberian lowlands (Podobina, 1998). Studies of ODP sites in the Norwegian-Greenland Sea provide a basis for establishing the taxonomical affinities of Arctic foraminifers with localities farther south. Miocene biostratigraphy at ODP Site 909 in Fram Strait was established by Osterman and Spiegler (1996); Kaminski and Austin (1999) studied the Oligocene at ODP Site 985 on the Iceland Plateau. The Eocene foraminiferal record is known from ODP Site 643 on the Vøring slope (Kaminski et al., 1990). The Cenozoic biostratigraphic record (mostly Paleocene to Miocene) of the North Sea and Labrador Sea was established by Gradstein et al. (1994). The stratigraphic record of agglutinated foraminifers in the Norwegian Sea area is continuous from the early Paleocene to the late Miocene, and with well over a hundred taxa reported from the area, this group provides good potential for stratigraphic correlation.

## Planktonic foraminifers

The standard low-latitude biostratigraphic zonation of Berggren et al. (1995) is not applicable to the Arctic region; therefore, direct correlations of planktonic foraminifers to the GPTS is not possible. Instead, comparisons were made with the regional biostratigraphy established at ODP sites in the Norwegian-Greenland Sea (Spiegler and Jansen, 1989; Spiegler, 1996) that make use of local planktonic foraminiferal first and last occurrences, coiling changes in *Neoglobobadrina*, and the biostratigraphic zonation.

tion of Weaver and Clement (1986). Unfortunately, the pre-Pliocene record of planktonic foraminifers in the Norwegian-Greenland Sea area is patchy at best and no biostratigraphic zonation exists for the area.

### Ostracodes

There is no formal biostratigraphic zonation for Cenozoic ostracodes from the Arctic Ocean; however, there are stratigraphic range data for many species found in widely scattered literature. Prior ODP legs have yielded preliminary information on Neogene ostracodes from the Vøring Plateau (Malz, 1989; Leg 104 Sites 642–644) and the Yermak Plateau (Cronin and Whatley, 1996; Leg 151 Sites 910 and 911). Both studies were of a preliminary nature, and no formal ostracode zonation was developed.

Outcrop exposures and shallow-water cores from the circum-Arctic and sub-Arctic regions in the North Atlantic and Pacific regions provide additional stratigraphic information on high-latitude northern hemisphere species (see Cronin et al., 1993, for a review). These studies include the Pliocene of the Alaska Coastal Plain (Repenning et al., 1987), the Pliocene–Pleistocene Iperk sequence in the eastern Beaufort Sea (Siddiqui, 1988), the Pliocene Kap Kobenhaven and Lodin Elv formations of Greenland (Brouwers et al., 1991; Penney, 1990, 1993), the Tjornes, Iceland, Pliocene–Pleistocene (Cronin, 1991), and Paleocene of West Greenland (Szczechura, 1971).

Shallow-water ostracode zonations for the Cenozoic of the British Isles (Keen, 1978), France (Oertli, 1985), and Germany and the Cenozoic of the deep North Atlantic (Coles and Whatley, 1989; Whatley and Coles, 1987) will also be useful in correlating Expedition 302 cores with other regions.

Previous coring in the deep Arctic Ocean has yielded abundant data on ostracodes from the last few glacial and interglacial cycles of the Quaternary (Cronin et al., 1994, 1995; Polyak et al., 2004). These studies show that ostracodes are highly sensitive to oceanographic changes related to Arctic water mass and sea-ice conditions.

Ostracodes were picked from the >150  $\mu\text{m}$  size fraction of the micropaleontological residue used for foraminiferal studies.

The following categories were used to describe ostracode abundance:

- A = abundant (>250 specimens).
- C = common (25–250 specimens).
- F = few (5–25 specimens).
- R = rare (1–5 specimens).
- B = barren (no specimen present).

### Palynology, organic-walled dinoflagellate cysts

In the absence of an established zonation scheme for the Arctic Ocean, the distribution pattern of index taxa is compared to the global Late Cretaceous–Cenozoic compilation of Williams et al. (2004). In addition, comparisons were made to relevant northern high-latitude studies, including those of Head and Norris (1989), Firth (1996), Williams and Manum (1999), and Eldrett et al. (2004).

Samples were processed on board using sodium hexametaphosphate, following the procedures described by Riding and Kyffin-Hughes (2004). “Heavy-liquid” ( $\text{ZnCl}_2$ ) separation was applied. Following sieving over a 20  $\mu\text{m}$  sieve, strewn mounts of the residue were made using glycerine jelly. Organic-walled dinoflagellate cysts (dinocysts) were counted to >100 specimens, whereas other major categories of palynomorphs (e.g., bisaccate pollen, spores, and foraminifer linings) were also taken into account. Dinocyst taxonomy is in accordance with that cited in Williams et al. (1998).

### Fish teeth

Although fish teeth have been used for biostratigraphy in the Pacific Ocean (e.g., Doyle and Riedel, 1979), we extracted ichthyoliths from the sediment primarily for the purpose of making geochemical measurements (e.g., Gleason et al., 2004, and references therein). Samples (20  $\text{cm}^3$ ) of raw sediment were disaggregated and sieved using only distilled water. Individual fish teeth were picked from the coarse residue and stored in a cardboard slide for each sample. These specimens were then further chemically cleaned prior to analysis according to the procedure of Gleason et al. (2004). The presence of other fossil fish material in Hole M0004A is shown in the foraminiferal occurrence table.

## Stratigraphic correlation Composite depths

The scientific objectives of Expedition 302 include examination of the sedimentary record at high resolution as well as recovery of a geological record that is as stratigraphically complete as possible. Core recovery from a single hole is insufficient to accomplish these goals because of recovery gaps between adjacent cores, even with a nominal 100% recovery. To obtain a complete sedimentary record, multiple adjacent holes are cored with an offset in depth of typically 1–2 m between cores from different holes to ensure that intervals missing in a single cored hole can be recovered from an adjacent hole.

Several aspects of Expedition 302 necessitate a modified approach toward hole-to-hole stratigraphic correlation and generation of composite depths compared to previous, non-MSP cruises. In particular, the shorter core length (~4.5 m at full recovery, compared to ~9.5 m with IODP) and a limited number of planned holes (two to three) make it more challenging to ensure complete overlap of cores. During Expedition 302, the main mode of stratigraphic correlation was actually a site-to-site correlation, as the drill sites are close to each other and are tied together confidently by seismic stratigraphy.

The offset in depth required in subsequent holes must rapidly be determined before and during coring. The continuity of recovery is assessed by developing composite sections that align prominent features in physical property data from adjacent holes. The procedure and rationale for this stratigraphic correlation is described in this section and follows the methodology pioneered during ODP Legs 94 (Ruddiman et al., 1987) and 138 (Hagelberg et al., 1992). Similar methods were employed and developed further during ODP Legs 154 (Curry, Shackleton, Richter, et al., 1995), 162 (Jansen, Raymo, Blum, et al., 1996), 167 (Lyle, Koizumi, Richter, et al., 1997), 171B (Norris, Kroon, Klaus, et al., 1999), and more recent ODP legs such as 199 (Shipboard Scientific Party, 2002; Pälike et al., 2005). During ODP Leg 202 it was found that vertical tidal movements can have a significant impact on the predicted meters below seafloor depth for a given stratigraphic interval (Shipboard Scientific Party, 2003). For Expedition 302, tidal movements were expected to be small, and this was confirmed pre-cruise for the anticipated drilling days and locations, with predicted tides of less than a few tens of centimeters (L. Erofeeva, pers. comm., 2004; Padman and Erofeeva, 2004).

### Data employed for stratigraphic correlation

Onboard stratigraphic correlation requires closely spaced data that can be generated rapidly. After each whole-core section had equilibrated to room temperature (typically 3–5 h), it was run through the custom-modified Geotek MSCL (see “[Petrophysics](#)”). The MSCL generates high-resolution (down to 2 cm intervals) measurements of magnetic susceptibility (MS), gamma ray attenuation (GRA) bulk density, *P*-wave velocity, and electrical resistivity (RES). Natural gamma radiation (NGR) and color reflectance data were not measured during the offshore phase and were instead measured during the onshore phase at BCR.

The MSCL was run in two separate modes: rapid and standard. In the rapid mode, the MSCL was run us-

ing two MS loops at a depth resolution of 2 cm; other parameters were measured at a depth resolution of 4 cm. The cores were measured quickly after retrieval, and their temperature may not have necessarily equilibrated with the laboratory temperature. Thus, the data are not absolute values of MS and were only used for initial offshore stratigraphic correlation. In the standard mode, all MSCL parameters (MS, bulk density, *P*-wave velocity, and RES) were measured at a depth resolution of 2 cm. As the core flow was lower than expected, both MS loops were used to measure susceptibility values at the same positions downcore. These duplicate measurements were used for quality control and were averaged where appropriate. The data files saved from the Geotek (version 7.3) software (both raw and processed) were copied across to a dedicated stratigraphic correlation computer via the network, where data from individual cores were assembled into a continuous downhole record with custom written conversion scripts. These scripts also attached mbsf depths for each measurement, as the output from the Geotek software is limited to downcore depths. For the detailed setup of the Geotek scanner, see “[Petrophysics](#).” During the coring operation, it became clear that geochemical data could be used for stratigraphic correlation purposes. Ammonia concentrations (see “[Geochemistry](#)”) were loaded into the stratigraphic correlation software and complemented the stratigraphic correlation process.

During the onshore phase, cores were run through an MSCL with an NGR emission sensor. NGR data were generated at 6 cm intervals and proved useful in the correlation of cores, with a distinct signal throughout the stratigraphic intervals recovered. In addition, measurements of color reflectance in the 400–700 nm wavelength range and calculated  $L^*a^*b^*$  values were made at a 5 cm depth resolution on the split archive half of the core using a Minolta spectrophotometer (see “[Petrophysics](#)”). The red-green parameter ( $a^*$ ), in particular, proved useful for correlation of distinct color changes between the lithologies.

Cores split longitudinally into working and archive halves during the onshore phase allowed for a detailed examination of core quality and verification of correlatable features. Cores were assessed for signs and levels of core disturbance, flow-in, and other coring-related features during the core description (see “[Lithostratigraphy](#)”) and line image color scanning phase. The results of these assessments are summarized on the barrel sheets (see “[Core Descriptions](#)”) in a Core Disturbance column. An example of the types of core disturbance encountered is given in Table [T2](#).



## Composite section development

IODP sample and core depths are recorded in mbsf from the first core in each hole that shows a true mudline, and consecutive depth measurements are determined by the length of the drill string. Several factors can lead to a deviation of the relative distance of geological features in the core from their true in situ stratigraphic separation. For example, sediment inside the core can expand as a result of reduced effective stress following core recovery, leading to an expanded sedimentary sequence relative to its original length (Moran, 1997). Thus, sediment can be missing between cores, even if a nominal 100% recovery is achieved. In addition, variations in ship motion, tides, and heave can result in stretching and/or squeezing of the recovered sediment in particular intervals and even multiple recovery of identical stratigraphic intervals in consecutive cores. To allow the placement of geological data from different holes according to their stratigraphic position, physical property measurements are correlated to create a meters composite depth (mcd) scale. The generation of a mcd scale attempts to match coeval stratigraphic features, as recorded by the MSCL and color reflectance measurements, at the same level by generating a composite record from different holes. This process requires depth shifting cores relative to each other. During this step, the total length on the mcd scale is typically expanded by 10% compared to the mbsf scale, although this factor can vary between ~5% and 15% (Hagelberg et al., 1992; Norris, Kroon, Klaus, et al., 1998). Site-to-site and hole-to-hole correlation was facilitated by using the graphical and interactive UNIX platform software, Splicer (version 2.2), which was developed by Peter deMenocal and Ann Esmay of the Lamont-Doherty Earth Observatory Borehole Research Group (LDEO-BRG) (available on the World Wide Web at [www.ldeo.columbia.edu/BRG/ODP](http://www.ldeo.columbia.edu/BRG/ODP)). Significant modifications were made for this expedition (by H. Pälike) to run the program on Mac OSX 10.3. The log-integration software Sagan was also modified.

Splicer allows data sets from adjacent holes to be correlated simultaneously, making use of interactive cross-correlation computation. After prominent features are aligned and referenced to a new mcd scale, a spliced record is generated by switching holes to avoid core gaps or disturbed sediment, resulting in a continuous record. Another output of the composite depth scale is generation of a template that forms the basis for sediment sampling along a complete section, thus minimizing duplicate sampling and saving analytical time. For this reason, it is highly desirable to apply a constant offset to an entire core such that the depth increments along individual

cores on the mcd scale are linearly related to the curated core depth increments. Splicer only allows the application of a constant offset for each core. However, composite depth scales created using the Splicer method are usually not satisfactory to create a stacked record from different holes because not every individual feature present across different holes can be aligned. Hence, if the aim is to increase the signal-to-noise ratio of quasi-periodic cycles that might be recorded in the sedimentary record, it is important to allow stretching and squeezing within individual sections so that data from different holes on the individual cycle level are aligned.

The procedure for generating a common depth scale that allows stretching and squeezing on a fine level was pioneered by Hagelberg et al. (1995) and results in a revised mcd (rmcd) common depth scale. Generation of rmcd scales is typically conducted as part of postcruise work. Composite depth generation using Splicer first begins by assigning the core with the best record of the upper few meters of a hole as the top of the composite record, and it typically contains the mudline. This core is assigned an mcd identical to its mbsf depth. A tie point, which gives the preferred correlation, is selected between data from this first core and a core in a second hole. All the data from the second hole below the correlation point are vertically shifted to align the tie points between the holes. After choosing an appropriate tie point and adjusting the depths, the shifted section becomes the next “reference” section and a tie is made to a core from the first hole. Working downhole in an iterative fashion, each core is then vertically shifted. Where there is no overlap, consecutive cores are appended. The tie points are recorded in a Splicer output (“affine”) table in units of mcd. The affine table that relates mbsf to mcd values along with the applied linear offsets for each core is presented in tabular form in “**Stratigraphic correlation**” in the “Sites M0001–M0004” chapter. A shortened composite depth table for Site M0004 is given as an example in Table T3. The last two columns in each table give, for each core, the cumulative depth offset added to the IODP curatorial subbottom depth (in mbsf) and the composite depth (in mcd), respectively. The depth offset column allows the calculation of the equivalent depth in mcd by adding the amount of offset listed to the depth in mbsf of a sample taken in a particular core. Table T4 shows a typical example for the Splicer file that defines the switching across holes to generate a spliced composite section. The composite depth and splice-tie point tables from each site chapter are also available in ASCII.

Figure F6 illustrates how creating a composite record allows alignment of the most prominent lithologic



features (example from Leg 199, Site 1218; Pälke et al., 2005). In the left panel, MS data from three holes at one site are shown on the mbsf depth scale, whereas in the middle panel, the data are shown on a common depth (mcd) scale together with a generated spliced record, indicating where the sample track was switched from one hole to the next. The right panel shows the rmcd scale, where individual physical property features were aligned by stretching and squeezing, together with a final stacked record from all holes. If the available data allow only an ambiguous or imprecise correlation or if multiple hole data were unavailable, no additional depth adjustments were made. In this case, the cumulative offset remains constant for all subsequent cores. On several occasions cores had a recovery >100% percent, resulting in overlapping mbsf depths. For these cores, we applied small vertical offsets to avoid overlap, while generally trying to keep mcd values close or identical to mbsf depths where there was no overlap between holes. Splice tie points were made between adjacent holes at identifiable, highly correlated features and were placed at transitions rather than peaks. Each splice was constructed beginning at the mudline at the top of the composite section and worked downward. Typically, one chooses one hole as the backbone for the record and cores from other holes are then used to patch in the missing intervals in core gaps (Fig. F6). Intervals were chosen for the splice such that section continuity was maintained, whereas disturbed intervals were avoided. The final alignment of the adjacent holes could be slightly different from the best overall visual or quantitative hole-to-hole correlation because of the constraint that a constant offset be applied to each core by the Splicer software.

### Technological advancements

During Expedition 302, it was important to use the stratigraphic correlation to make coring decisions in near real time. This was achieved by introducing several modifications to the standard IODP protocol. Crossover between shifts was done over the Internet connection (mirroring the correlation computer screen between ships). Stratigraphic correlators were able to view the status of the splice on computers while they talked by mobile telephone between the drilling vessel *Vidar Viking* and the operations center vessel *Oden*.

In addition to the MSCL data, lower-resolution core catcher sample data (age, grain size, color, and density) were used to support this work. Scientists aboard *Oden* provided these supplemental data by regularly updating an Excel spreadsheet with this information on the central server, which was available

across vessels by means of wireless data transfer and networking. A faster throughput of cores through the MSCL was achieved by incorporating two MS loops calibrated and run at slightly different frequencies.

## Petrophysics

The primary objective of the petrophysical program was to collect high-resolution data to

1. Allow hole-to-hole correlation and facilitate the retrieval and construction of a complete composite stratigraphic section,
2. Provide data for construction of synthetic seismograms to allow near-real-time tracking of drilling progress and to investigate the characteristics of major seismic reflectors, and
3. Provide data for characterization of lithologic units.

Petrophysical measurements were either performed on whole cores and discrete samples or were made in situ through wireline logging or specialized down-hole tools. The bulk of the petrophysical program was associated with collecting high-resolution, non-destructive measurements on whole cores using the Geotek MSCL. While offshore, the MSCL was outfitted with four sensor types capable of measuring bulk density, MS, transverse compressional wave (*P*-wave) velocity, and RES (see “[Stratigraphic correlation](#)”). The MSCL was used onshore to acquire digital line scan images, measure *P*-wave velocity on selected sections where whole-core measurements performed offshore resulted in poor quality data, and measure bulk density and MS on one core (302-M0004C-6X) that was too thick to fit through the MS loops offshore.

Lower-resolution MAD, shear strength, color reflectance, and needle-probe thermal conductivity measurements were also routinely performed. A helium gas pycnometer was used to measure the volume (for density determinations) of discrete samples taken from the core catchers of each core while offshore and at an approximate resolution of one per section from the working half of split cores at BCR. This allowed an independent determination of bulk density, grain density, water content, porosity, and void ratio, which were used to calibrate the high-resolution, nondestructive measurements made with the MSCL.

In situ temperature measurements were made with two different tools, the Adara tool (from ODP) and a BGS-supplied tool.

In situ petrophysical measurements were also obtained using a single wireline tool string (Fig. F7).

The tool string measured microresistivity using the Formation MicroScanner (FMS), *P*-wave velocity using the Borehole Compensated Sonic (BHC) tool, total NGR emissions using the Scintillation Gamma Ray Tool (SGT), and spectral emissions using the Natural Gamma Ray Spectrometry Tool (NGT).

### MSCL measurements

The principal aim of MSCL data acquisition during the offshore component of Expedition 302 was to obtain high depth-resolution data sets to facilitate shipboard core-to-core correlation during construction of composite stratigraphic sections. The MSCL was run in two separate modes: rapid and standard. In rapid mode, the MSCL could be run using two MS loops, both set at a resolution of 4 cm. Because the loops would measure out of sequence with one another, the resulting MS data had a downcore resolution of 2 cm. In rapid mode, cores were run quickly and were not necessarily equilibrated to laboratory temperature. In standard mode, both MS loops performed susceptibility measurements in conjunction with GRA density, *P*-wave velocity, and resistivity measurements. Standard resolution for all instruments was 2 cm. Standard mode measurements were performed on temperature-equilibrated cores. Cores that were to be sampled for geochemistry and microbiology were all logged in rapid mode prior to removing whole rounds, samples, or pore water (see “[Geochemistry](#)”). Sampled cores were subsequently logged in standard mode, and correlation between rapid and standard modes will be used to correct the rapid-logged data if deemed necessary. All MSCL data included in this volume are from standard-mode logging.

### MSCL measurement principles

#### Magnetic susceptibility

Whole-core MS was measured with the MSCL using two Bartington MS2 meters and MS2C loop sensors. The MS2C loop sensors had an internal diameter of 80 mm, which corresponds to a coil diameter of 88 mm. It normally operates at a frequency of 0.565 kHz and an alternating-field (AF) intensity of 80 A/m (= 0.1 mT). During the offshore component of Expedition 302, two Bartington loops were installed on the MSCL to enable rapid core logging. The necessity for rapid logging originated from the need to have near real-time stratigraphic correlations to help guide drilling decisions. In order to have two sensors operating concurrently without interference, their operating frequencies were offset. MS1 was set to an operating frequency of 621 Hz, and MS2 was set at 513 Hz. Correction factors for each of the sensors (1.099× for MS1 and 0.908× for MS2) were used to

adjust the values equivalent to measurement at the standard 565 Hz. Calibration standards with bulk susceptibility ( $\chi$ ) of  $210 \times 10^{-6}$  cgs (MS1) and  $213 \times 10^{-6}$  cgs (MS2) were used to check the operation of each susceptibility sensor. The MSCL software automatically corrected the MS data for the dual operating frequencies in the processed data output.

The MS2C meter operates on two sensitivity levels, 0.1× and 1×, which correspond to a 10 s and 1 s sampling period, respectively. The higher sensitivity setting results in measurements to the first decimal place, with the 10-fold increase in measurement time providing additional noise filtering. The resolution of the loop is  $2 \times 10^{-6}$  SI on the 0.1 range (10 s measuring time). The effective sensor length of the 80 mm MS2C loop is 4 cm. During offshore Expedition 302, MS measurements were routinely made at a spacing of 2 cm, with a single data acquisition made on the 1× range. MS data were archived as raw instrument units and were not corrected for changes in sediment volume.

#### Density

Bulk density is estimated by measuring the attenuation of gamma rays that have passed through the cores, with the degree of attenuation being proportional to density (Boyce, 1976). Calibration of the system was completed using known seawater/aluminum density standards (see Blum, 1997). Bulk density data are of highest quality when determined on APC cores because the liner is generally completely filled with sediment. In XCB cores, density measurements are of lower quality and cannot necessarily be used to reliably determine bulk density on their own. The measurement length of the GRA sensor is ~0.5 cm, with sample spacing set at 2 cm during offshore Expedition 302. The minimum integration time for a statistically significant GRA measurement is 1 s; routine GRA measurements were run at a 4 s integration time.

#### *P*-wave velocity

Transverse *P*-wave velocity was measured on the MSCL with the *P*-wave logger (PWL). All cores where sediment and liner coupling existed and saturation was high enough to transmit the pulse were measured. The PWL transmits a 500 kHz compressional wave pulse through the core at 1 kHz. The transmitting and receiving transducers are aligned perpendicular to the core axis. A pair of displacement transducers monitors the separation between the compressional wave transducers so that variations in the outside diameter of the liner do not degrade the accuracy of the measured velocities. Repeated measurements of *P*-wave velocity through a core liner

filled with distilled water were used to calibrate the offsets in traveltime that occur through the system components and core liner. The measurement width of the PWL sensor is ~0.1 cm, with sample spacing routinely set at 2 cm for Expedition 302 measurements.

### Electrical resistivity

Electrical RES of sediment cores was measured using the noncontact resistivity (NCR) sensor on the MSCL. NCR measurements are made using a high-frequency magnetic field to induce an electrical current in the core. Magnetic fields, generated by the induced electrical current, are measured on a receiver coil and normalized with a third set of coils operating in air. The NCR is calibrated by measuring the resistivity of five standard 0.45 m core liner sections containing water of varying but known salinity and relating the known resistivity of each stock solution with the millivolt output from the meter. Standards were made by mixing a 7 L stock solution of 35,000 ppm NaCl distilled water. Dilution of the stock solution allowed five standards to be made with concentrations of 35,000, 17,500, 3,500, 1,750 and 350 ppm. By measuring the standards on the MSCL, an exponential regression was fit between resistivity (ohm-meters) and sensor output in millivolts. Values from the regression were entered into the MSCL software and applied internally to the raw sensor readings.

### Natural gamma radiation

NGR emissions of sediments are a function of the random and discrete decay of radioactive isotopes, predominantly those of  $^{238}\text{U}$ ,  $^{232}\text{Th}$ , and  $^{40}\text{K}$ , and are measured through scintillation detectors housed in a shielded collector. For the onshore phase of Expedition 302, a Geotek frame system was employed that allowed up to six cores to be logged during a single run. The gamma ray detector has a measurement window of 7.5 cm, and the sampling interval was set at 6 cm, in order to maximize the resolution of measurements while minimizing resampling of intervals. The count time at each sampling point was set at 4 min. This sampling interval and count time provided the highest resolution and best data quality possible within the time available to complete the core logging. The increased counting times required whole-core gamma ray logging to start 2 weeks prior to the arrival of the science party in Bremen, being completed at the end of the first week of the onshore phase. The data are presented as total counts per second and refer to the integration of all emission counts over the gamma ray energy range between 0 and 3 MeV and is best suited for core-to-core correlation. No corrections were made to NGR data to ac-

count for volume effects related to sediment incompletely filling the core liner.

### Digital color imaging system

While onshore, systematic high-resolution line-scan digital core images of the archive half of each core were obtained using the Geotek X-Y digital imaging system (Geoscan II). This system collects digital images with three line-scan charge-coupled device arrays (1024 pixels each) behind an interference filter to create three channels (red, green, and blue [RGB]). The image resolution is dependent on the height of the camera and width of the core. The standard configuration for the Geoscan II produces 300 dots per inch (dpi) on an 8 cm wide core, with a zoom capability up to 1200 dpi on a 2 cm wide core. Synchronization and track control are better than 0.02 mm. The dynamic range is 8 bits for all three channels. The framestore card has 48 MB of onboard random access memory (RAM) for acquisition of images with an ISA interface card for personal computers. The system was calibrated at the start of each day. Output from the digital imaging system includes a Windows bitmap (.BMP) file and a compressed (.JPEG) file. The bitmap file contains the original data with no compressional algorithms applied. All cores were imaged using an aperture setting of f/5.6 except Cores 302-M0002A-52X and below in Hole M0002A (imaged using both f/5.6 and f/4) and Cores 302-M0004A-6X and below in Hole M0004A, which were imaged using f/4. RGB curves were produced for undisturbed core sections by averaging across a 2 cm wide strip (4.5–6.5 cm) at an interval of 2 mm downcore. When utilizing the RGB data it is recommended that detailed examination of core photographs/images and disturbance descriptions/tables is undertaken in order to cull unnecessary or spurious data.

### Diffuse color reflectance spectrophotometry

Archive halves were measured at 5 cm intervals using a handheld Minolta spectrophotometer (model CM-2600d). Black and white calibration of the spectrophotometer was performed every 24 h. Prior to measurement, the core surface was scraped and covered with a clear plastic wrap to maintain a clean spectrometer window.

Spectrophotometric analysis produced three types of data: (1)  $L^*$ ,  $a^*$ , and  $b^*$  values, where  $L^*$  (lightness) is a total reflectance index ranging from 0% to 100%,  $a^*$  is the green (–) to red (+) chromaticity, and  $b^*$  is the blue (–) to yellow (+) chromaticity; (2) Munsell color values; and (3) intensity values for 31 contiguous 10 nm wide bands across the 400 to 700 nm interval of the visible light spectrum.

Measurements were not performed on severely disturbed intervals, particularly in regions containing slurry and flow-in. Measurements on cores with biscuiting and rough surfaces slightly biased the digital and spectrophotometric data toward darker values. When utilizing the spectrophotometric measurements it is recommended that detailed examination of core photos/images and disturbance descriptions/tables is undertaken in order to cull unnecessary or spurious data.

### Moisture and density

MAD (bulk density, grain density, water content, porosity, and void ratio) was determined from measurements of wet and dry sediment mass and dry sediment volume. Offshore, constant-volume samples of  $\sim 4.56 \text{ cm}^3$  were taken from core catchers that were brought aboard the *Oden* from the *Vidar Viking*. In general, one MAD sample from each core catcher was taken. Discrete samples were also taken from the working half of split cores at BCR. Onshore MAD sampling was at a resolution of  $\sim 1$  per section.

Sample mass was determined using the marine analytical balance and associated Core Logic software. The balance was equipped with a computer averaging system that corrected for ship acceleration. The sample mass was counterbalanced by a known mass so that the mass differential was generally  $< 1 \text{ g}$ . After drying the sediment samples at  $105^\circ\text{C}$  for 24 h and weighing to determine the dry sediment mass, the samples were crushed using a mill grinder. Subsamples of  $\sim 3.6 \text{ cm}^3$  from the crushed sediment were weighed and prepared to determine volume using Micrometrics Accupyc 1330 pycnometer, a helium-displacement pycnometer capable of measuring one sample per run. The volume measurements were repeated five times by the pycnometer software until the last two measurements exhibited  $< 0.01\%$  standard deviation. A reference volume consisting of a  $36.0604 \text{ g}$  tungsten sphere was used on several occasions to check the instrument for drift and systematic errors.

Onshore, discrete samples were extracted from the working half of split cores ( $\sim 1$  per section) and placed in  $10 \text{ mL}$  beakers where core recovery allowed. Sample mass was determined to a precision of  $0.001 \text{ g}$  using an electronic balance. Sample volumes were determined using a Quantachrome penta-pycnometer (helium-displacement pycnometer) with a precision of  $0.02 \text{ cm}^3$ . Volume measurements were repeated a maximum of five times, or until the last three measurements exhibited  $< 0.01\%$  standard deviation. A reference volume was included within each sample set and rotated sequentially among the cells to check for instrument drift and systematic er-

ror. A purge time of 1 min was used before each run. Dry mass and volume were measured after samples were heated in an oven at  $105^\circ \pm 5^\circ\text{C}$  for 24 h and allowed to cool in a desiccator. The procedures for determination of MAD are described in the offshore phase of the methods above and are not repeated here. The procedures for determination of MAD comply with the American Society for Testing and Materials (ASTM) designation (D) 2216 (ASTM, 2005).

Wet mass ( $M_{\text{wet}}$ ), dry mass ( $M_{\text{dry}}$ ), and dry volume ( $V_{\text{dry}}$ ) were measured in the laboratory. Salt precipitated in sediment pores during the drying process is included in the  $M_{\text{dry}}$  and  $V_{\text{dry}}$  values. The mass of the evaporated water ( $M_{\text{water}}$ ) and the salt ( $M_{\text{salt}}$ ) in the sample are given by

$$M_{\text{water}} = M_{\text{wet}} - M_{\text{dry}} \text{ and} \\ M_{\text{salt}} = M_{\text{water}} [s/(1 - s)],$$

where  $s$  = assumed seawater salinity ( $0.035$ ) and corresponds to a pore water density ( $\rho_{\text{pw}}$ ) of  $1.024 \text{ g/cm}^3$  and a salt density ( $\rho_{\text{salt}}$ ) of  $2.257 \text{ g/cm}^3$ . The corrected mass of pore water ( $M_{\text{pw}}$ ), volume of pore water ( $V_{\text{pw}}$ ), mass of solids excluding salt ( $M_{\text{solid}}$ ), volume of salt ( $V_{\text{salt}}$ ), volume of solids excluding salt ( $V_{\text{solid}}$ ), and wet volume ( $V_{\text{wet}}$ ) are, respectively,

$$M_{\text{pw}} = M_{\text{water}} + M_{\text{salt}} = M_{\text{water}}/(1 - s), \\ V_{\text{pw}} = M_{\text{pw}}/\rho_{\text{pw}}, \\ M_{\text{solid}} = M_{\text{dry}} - M_{\text{salt}}, \\ V_{\text{salt}} = M_{\text{salt}}/\rho_{\text{salt}}, \\ V_{\text{solid}} = V_{\text{dry}} - V_{\text{salt}} = V_{\text{dry}} - M_{\text{salt}}/\rho_{\text{salt}}, \text{ and} \\ V_{\text{wet}} = V_{\text{solid}} + V_{\text{pw}}.$$

For all sediment samples, water content ( $w$ ) is expressed as the ratio of the mass of pore water to the wet sediment (total) mass,

$$w = M_{\text{pw}}/M_{\text{wet}}.$$

Bulk density ( $\rho$ ), sediment grain density ( $\rho_g$ ), and porosity ( $n$ ) are calculated from:

$$\rho = M_{\text{wet}}/V_{\text{wet}}, \\ \rho_g = M_{\text{solid}}/V_{\text{solid}}, \text{ and} \\ n = V_{\text{pw}}/V_{\text{wet}}.$$

### Shear strength

Undrained shear strength ( $S_u$ ) of sediments was measured using three devices, the Torvane, pocket penetrometer, and a fall cone. Offshore, measurements of shear strength were performed on each core, at either the top or the bottom of an undisturbed, freshly cut section aboard the *Vidar Viking*. Both the Torvane and the pocket penetrometer are handheld devices that allow for rapid determination of strength in cohesive sediment. The pocket penetrometer is more



effective when sediments become slightly indurated, whereas the Torvane, equipped with two heads, allows determination of shear strength in weakly and moderately indurated sediments.

The Torvane is a small, handheld, spring-loaded device with a vane blade that is pressed into the sample and turned. Strength measurements made with the Torvane are affected by changes in the amount of pressure applied to the device and the rate of rotation. The rotation rate is supposed to cause failure of the sediments within 5 to 10 s. A scale on the dial reads the approximate shear strength of the sample, with the smallest division being 0.05 t/ft<sup>2</sup> (488.24 kg/m<sup>2</sup>). Similar to the automated vane shear tests,  $S_u$  determinations using the handheld Torvane assume that a cylinder of sediment is uniformly sheared around the axis of the vane and remains in an undrained condition during the test. In this state, cohesion is the principal contributor to the shear strength. Violation of this assumption occurs with progressive cracking of the failing specimen, drainage of local pore pressures (i.e., the test can no longer be considered undrained), and stick-slip behavior.

The pocket penetrometer measures the unconfined compressive strength of sediments, which, in an ideal clay, is equal to twice  $S_u$  (Holts and Kovacs, 1981). Measurements are made by pressing the retracting head of the penetrometer into the end of the core. The amount of force required to press the head 5 mm into the sediment is read on a calibrated scale. The maximum shear strength measurable with the pocket penetrometer is 245 kPa.

Onshore,  $S_u$  measurements were made using a fall-cone device. The fall cone measures the penetration of a standard cone as it free falls a set distance and embeds itself into the sediment. During testing, the cone is lowered so that it just touches and marks the surface of the split core before it is locked in place with the dial gauge reading noted. The cone is then released and penetrates the surface of the sample. A single cone was used during Expedition 302 which had an apex angle of 30° and a mass of 80.5 g. The undrained shear strength is determined using an empirical formula determined by Hansbo (1957), where

$$S_u = K \times M/d^2,$$

where

- $S_u$  = undrained shear strength (kPa),
- $K$  = empirical factor related to the cone angle and sediment type,
- $M$  = weight of the cone (N), and
- $d$  = penetration distance of cone (mm).

A  $K$  factor, which is dependent on the apex angle of the cone, of 0.85 was used and was determined based

on common  $K$  factors used in the literature (Zreik, 1995).

## Thermal conductivity

Thermal conductivity was measured with the TeKa TK04 system using the needle-probe method in full-space configuration for soft sediments (Von Herzen and Maxwell, 1959). The needle probe contains a heater wire and calibrated thermistor. It is assumed to be a perfect conductor because it is much more conductive than the unconsolidated sediments that it is measuring. Cores were brought into the laboratory and allowed to equilibrate to room temperature, which took ~4 h. Thermal conductivity was then measured by inserting the needle probe into the sediment through a small hole drilled into the core liner. Generally, thermal conductivity ( $k$ ) is calculated from the following:

$$k(t) = (q/4\pi) \times \{[\ln(t_2) - \ln(t_1)]/[T(t_2) - T(t_1)]\},$$

where

- $T$  = temperature,
- $q$  = heating power (heat input per unit length per unit time), and
- $t_1, t_2$  = time interval along the heating (normally 80 s duration) curve.

The correct choice of  $t_1$  and  $t_2$  is complex; commonly, thermal conductivity is calculated from the maximum interval ( $t_1$  and  $t_2$ ) along the heating curve where  $k(t)$  is constant. In the early stages of heating, the source temperature is affected by the contact resistance between the source and the full space and in later stages is affected by the finite length of the heating source (assumed infinite in theory). The special approximation method (SAM), employed by the TK04 software, is used to develop a best fit to the heating curve for all of the time intervals where

$$20 \leq t_1 \leq 40,$$

$$45 \leq t_2 \leq 80, \text{ and}$$

$$t_2 - t_1 > 25.$$

A good measurement results in a match of several hundred time intervals along the heating curve. The best solution is the one that most closely corresponds to the theoretical curve, and this is the output thermal conductivity. Three to five measuring cycles were automatically performed at each sampling location and, when obtained, the closest three were used to calculate an average thermal conductivity. Thermal conductivity measurements were taken with a frequency of one per core (section 2 where available) in soft sediments, into which the TK04 needles could be inserted without risk of damage.

## In situ temperature measurements

In situ temperature measurements were made with either the Adara tool, developed by ODP, or the BGS temperature probe. The Adara tool consists of electronic components mounted to a cylindrical metal frame that fits inside a cavity in the wall of the APC cutting shoe. An embedded operating system runs the electronics and can be connected via serial interface to a PC. During Expedition 302, the tool was deployed on the end of the extended corer. The core barrel with extension subs extended the Adara 1.5 m beyond the drill bit. During operation, the coring shoe is attached to the core barrel and lowered down the pipe by wireline. The tool is typically held for 10 min at the mudline to equilibrate with bottom water temperatures before being lowered to the end of the drill string. The thermal time constant of the cutting shoe assembly into which the Adara tool is inserted is ~2–3 min, and this was pushed down into the formation and held in place for ~20 min while temperature data were recorded. The Adara tool is left in the sediment for 10 min to obtain a temperature record that provides a sufficiently long transient record for reliable extrapolation of the steady-state temperature. A second stop for 10 min at the mudline is often made before raising the core barrel to the surface. Thus, a typical Adara measurement consists of a mudline temperature record lasting 10 min, followed by a pulse of frictional heating when the barrel is pushed into the sediment, a period of thermal decay that is monitored for 20 min, and a frictional pulse upon removal from the sediment. Before reduction and drift corrections, nominal accuracy of Adara temperature data is estimated at 0.1°C. Extrapolation of the temperature decay curves to in situ steady-state conditions were made postcruise.

The BGS temperature tool consisted of a small pressure housing containing a sensor and logging assembly, similar to the Adara cutting shoe tool. The tool is based on a microprocessor module and is accurate to 0.01°C. The microprocessor is embedded in a pressure housing, ~35 mm in diameter, and attached to the lower end of a core barrel and pushed into the sediment below the BHA. The tool deployment procedure used when running the Adara was adopted for measurements made with the BGS probe.

## Downhole logging

Downhole logging may be used to determine physical, compositional, and structural properties of the formation surrounding a borehole. Data are rapidly collected, continuous with depth, and measured in situ; they can be interpreted in terms of stratigraphy, lithology, mineralogy, and geochemical composition

of the penetrated formation. Where core recovery is incomplete or disturbed, logging data are useful for characterizing the borehole section. Where core recovery is good, logging and core data complement one another and may be interpreted jointly. Logging results are sensitive to formation properties on a scale intermediate between laboratory measurements on core samples and geophysical surveys.

Logs are recorded using a suite of tools that can be combined, one on top of another, to form a tool string capable of being lowered down an open hole. Data recorded by the tools are transferred to the shipboard acquisition system in real time by way of a wireline. A list of tools used during Expedition 302 and their associated measurements are shown in Table T5, and common logging acronyms are given in Table T6. The single tool string used during Expedition 302 combined the FMS, BHC, SGT, and NGT and is shown in Figure F7.

## Tool measurement principles

The properties measured by the tools and the principles of measurement are briefly described below. More detailed information on individual tools and their geological applications are found in Ellis (1987), Goldberg (1997), Lovell et al. (1998), Rider (1996), Schlumberger (1989, 1994), and Serra (1984, 1986).

### Natural radioactivity

The NGT was used to measure natural radioactivity in the formation. The NGT uses a sodium iodide scintillation detector and five-window spectroscopy to determine concentrations of the three elements whose isotopes dominate the natural radiation spectrum: potassium (in weight percent), thorium (in parts per million), and uranium (in parts per million). NGT response is sensitive to borehole diameter and can vary with drilling mud composition. During Expedition 302, the drill mud type was guar gum, which does not influence NGT response.

### Acoustic velocity

The BHC applies the “depth-derived” borehole compensation principle using two transmitter (1×) receiver (2×) groups, one group being inverted. The distance between the transmitter and the receivers is 3 and 5 ft, respectively. Hole size compensation is obtained by averaging the two compressional wave delay time ( $\Delta T$ ) readings measured across the same interval. Only compressional wave velocities are recorded by the BHC.

### Formation MicroScanner (FMS)

The FMS provides high-resolution electrical-resistivity-based images of borehole walls. The tool has four orthogonal arms (pads), each containing 16 micro-electrodes, or buttons, which are pressed against the borehole wall during the recording. The electrodes are arranged in two diagonally offset rows of eight electrodes each and are spaced ~2.5 mm apart. A focused current is emitted from the four pads into the formation, with a return electrode near the top of the tool. Array buttons on each of the pads measure the current intensity variations. Data processing transforms these measurements, which reflect the microresistivity variations of the formation, into continuous, spatially oriented, high-resolution images that mimic geologic structures behind the borehole walls. Further processing can provide measurements of dip and direction (azimuth) of planar features in the formation. Features such as bedding, fracturing, slump folding, and bioturbation can be resolved.

The maximum extension of the caliper arms is 15.0 inches. In holes with a diameter >15 inches, the pad contact can be inconsistent, resulting in blurred FMS images. Irregular borehole walls will also adversely affect the images, as contact with the wall is poor.

### Accelerometry and magnetic field measurement

Three-component acceleration and magnetic field measurements were made with the General Purpose Inclinerometer Tool. The primary purpose of this tool, which incorporates a three-component accelerometer and a three-component magnetometer, is to determine the acceleration and orientation of the FMS-sonic tool string during logging. Thus, the FMS images can be corrected for irregular tool motion, and the dip and direction (azimuth) of features in the FMS image can be determined.

### Logging data quality

The principal influence on logging data quality is the condition of the borehole wall. If the borehole diameter is variable over short intervals, resulting from washouts during drilling, clay swelling, or borehole wall collapse, the logs from tools that require good contact with the borehole wall (i.e., FMS) may be degraded. Deep investigation measurements such as sonic velocity, which do not require contact with the borehole wall, are generally less sensitive to borehole conditions. Very narrow stratigraphic sections will also cause irregular logging results. Borehole quality is improved by minimizing the circulation of drilling fluid, flushing the borehole to remove de-

bris, and logging as soon as possible after drilling and conditioning are completed.

### Logging depth scales

The depth of logging measurements is determined from the length of the logging cable played out from the winch on the ship. The seafloor is identified on the NGR log by the abrupt reduction in gamma ray counts at the mudline. The coring depth (mbsf) is determined from the known length of the BHA and pipe stands; the mudline is usually recovered in the first core from the hole. Discrepancies between coring depth and wireline logging depth occur because of core expansion, incomplete core recovery, incomplete heave compensation, drill pipe stretch, cable stretch (~1 m/km), and cable slip. Because of the damping effect of the sea ice, no heave compensation was required during Expedition 302.

The small but significant differences between drill pipe depth and logging depth should be taken into account when using the logs for correlation between core and logging measurements. Core measurements such as susceptibility and density can be correlated to the equivalent downhole logs using the Sagan program, which allows shifting the core depths onto the logging depth scale. Precise core-logging depth matching is difficult in zones where core recovery is low because of the inherent ambiguity of placing the recovered section in the cored interval. Distinctive features recorded by the NGT provide correlation and correction of relative depth offsets between the logging runs.

## Geochemistry

Relatively few geochemical measurements were made during the offshore component of Expedition 302. By contrast, numerous geochemical and mineralogical analyses were made during (and after) the onshore component. However, most of the ensuing geochemical data sets remained incomplete for weeks to months after the onshore component was terminated. Consequently, only the shipboard results could be submitted and discussed in the original draft of this volume.

We raise this issue for three reasons. First, it explains the flow of this discussion, where we have retained the “original” shipboard results and discussion at the beginning and subsequently add shore-based results and discussion. Second, it explains the fairly brief discussion of the results. Third, future MSP expeditions might consider alternative strategies for the onshore geochemical program. The primary problem encountered during Expedition 302 was the signifi-

cant time lag between collecting sediment samples down cores, processing and analyzing these samples in limited batches, and then collating and checking results. We chose to maximize our productivity, which meant collecting or processing samples while awaiting analytical results and which resulted in a large number of analyses. As alternative strategies, the total number of samples could have been decreased (but with significant idle time), the samples could have been collected and processed before the onshore component commenced (which was partly done using available core catcher and squeeze-cake samples), or the geochemical program could have been staggered after other onshore efforts (particularly the opening of cores, description of the lithology, and collecting of samples).

### Background and overall program

For nearly 20 y, well-established procedures were used to collect and analyze gases and pore waters from sediments aboard the *JOIDES Resolution* (Kvenvolden and McDonald, 1986; Gieskes et al., 1991). Although the “shipboard geochemistry” routine evolved with additional equipment (e.g., an inductively coupled plasma–atomic emission spectrometer, Murray et al., 2000) and new priorities (e.g., high-resolution sampling, D’Hondt, Jørgensen, Miller, et al., 2003), core flow and analytical methods remained essentially the same. There was also a growing tendency to measure an increasing number of chemical species (in both gas and water) in shipboard laboratories.

Sediment core, laboratory space, and scientific personnel were at a premium during Expedition 302. Recovery of a continuous sediment record was the highest scientific priority. This meant that the traditional cutting of whole-round samples from unexamined cores was not permitted. Laboratory space for chemistry on the drillship *Vidar Viking* was limited to less than half of a 5.5 m × 2.2 m container. This meant that only one person per shift could collect, prepare, and analyze gases and pore waters on the drilling vessel. The Expedition 302 shipboard geochemistry program documented below, therefore, has significant modifications from those of previous international scientific drilling expeditions (i.e., DSDP and ODP legs and IODP expeditions). Key differences include (1) water samples were taken after a core was logged, (2) most analyses were postponed to shore-based activities, (3) samples collected were transferred to the ice-breaker *Oden* for curation, and (4) shipboard analyses were conducted using different procedures. The overarching theme was to collect and appropriately store a sufficient number of samples to meet

IODP and shore-based needs while enabling construction of a continuous sediment section.

### Gas analyses

Two samples (HS-1 and HS-2) were collected for headspace gas analyses at selected depth intervals. A “pencil-sized” syringe (soft sediment) or cork borer (hard sediment) was inserted into the working-half end of a freshly exposed core section. After withdrawing the syringe or cork borer, a small amount of sediment was pushed out. This excess was shaved off with a flat spatula so that a sediment volume of 5 mL was obtained.

The two 5 mL sediment borings were extruded into 20 mL glass vials filled with 10 mL of seawater. Both headspace samples were immediately sealed with a septum and metal crimp cap, shaken for 2 min, and turned upside down to prevent gas loss. The samples were stored at room temperature on *Vidar Viking* and then transferred to *Oden*.

After 23.5 h, the first headspace sample was heated to 60°C for 20 min. A 1 mL volume of headspace gas was extracted from the vial using an Agilent glass syringe, which was not ideal. The gas volume was injected directly into a portable Agilent 6850 series gas chromatograph (GC) equipped with a 30 m × 0.536 mm stainless steel column packed with GS-Q stationary phase (Agilent 1153432) and a flame ionization detector (FID). Unfortunately, an appropriate calibration standard was not shipped, and the hydrogen carrier gas was exhausted after a few samples. Thus, no shipboard gas analyses are reported.

The second gas sample was frozen for shore-based gas analyses. At BCR, a 1 mL volume of headspace gas was extracted from each vial using a Hamilton gas-tight syringe. This volume was then injected directly into a Thermo-Finnegan trace GC equipped with a 30 m × 0.32 mm AT-Q capillary column and an FID. The carrier gas was helium, and the GC oven was programmed as follows: initial temperature of 90°C, held for 3 min, increased to 110°C over 1 min, held for 6 min, increased to 190°C over 5.3 min, held for 9 min, increased to 220°C over 2 min, and held for 4 min. The retention time for methane was 1.94 min. Data were collected using ChromQuest software. The instrument was calibrated by injecting known volumes of pure methane and pure ethane.

### Interstitial water samples

Shipboard interstitial water (IW) samples were collected by two methods: (1) high-pressure squeezing of whole-round intervals (Fig. F8) and (2) Rhizone sampling of intact cores (Fig. F9). Notes regarding



both methods are contained in the “Bremen Core Curation Van Handbook.” High-pressure squeezing has been commonplace during most sediment coring expeditions of DSDP, ODP, and IODP. Unfortunately, this procedure destroys the integrity of the sediment core. Rhizone sampling offers an alternative, nondestructive approach for collecting pore waters. However, it was not clear whether this method (Seeberg-Elverfeldt et al., 2005) could extract sufficient quantities of water, especially from indurated sediment. The goals of Expedition 302 provided a good rationale for developing and assessing this new method.

Whole-round intervals for squeezing were usually taken every third or fourth core. Approximately 5–10 cm long intervals were cut from sections in the laboratory after they passed through the MSCL. This procedure diverged significantly from standard ODP protocol, where samples are cut from cores on the catwalk before sectioning and MSCL analyses. However, it ensured that IW samples were taken only after collection of their sedimentary record. A potential disadvantage is that the time between core retrieval and squeezing was 30–40 min longer during Expedition 302 than during typical ODP legs. However, we doubt that this time lag significantly modified pore water chemistry (at least relative to IW collection on previous expeditions) because the low temperatures of the shallow-water column and ship deck would help to preserve water chemistry.

Each whole-round interval was extruded onto a stainless steel tray, where its surface was carefully scraped with a spatula to remove potential contamination. The remaining “sediment plug” was then placed into a titanium squeezer, which is detailed in the “Bremen Core Curation Van Handbook.” Pressures as high as  $10 \times 10^4$  N (gauge) were applied using the accompanying hydraulic press. Interstitial water was passed through a Whatman no. 1 filter fitted above a titanium screen, a hole in the base of the squeezer, and a  $0.45 \mu\text{m}$  disposable filter and into a 20 or 50 mL plastic syringe.

After IW collection, the syringe was removed from the squeezing apparatus and used to dispense IW aliquots. These aliquots included the following:

- 1.0 mL untreated for *Viking*-based salinity;
- 3.0 mL untreated for *Viking*-based pH and alkalinity;
- 2.0 mL untreated in plastic scintillation vials for *Oden*-based  $\text{NH}_4^+$ ;
- 8.0 mL in glass vials to be split on *Oden* for shore-based measurements of anions (e.g.,  $\text{SO}_4^{2-}$ ), sulfide and sulfur isotopes (2 mL saturated zinc acetate solution added to 2 mL of pore water), and  $^{13}\text{C}$  (1

drop of saturated  $\text{HgCl}_2$  solution added to 2 mL of pore water);

- 5 mL untreated for shore-based  $\text{Cl}^-$  and stable isotope analyses;
- 5 mL untreated as an archive sample; and
- 5 mL untreated for shore-based dissolved organic carbon (DOC) analyses.

Ideally, ~30 mL of pore water was taken to meet all requirements. In the case of excess pore water, additional archive samples were made; usually less water was collected, and the priority for making aliquots generally followed the order listed above.

For Rhizone sampling, cores were logged, placed in a rack, and turned so the cutting line was vertical. From one to four holes were drilled through the liner on the top of the working half. Rhizones were then fully inserted into the sediment and connected to evacuated 10 mL syringes. Even with four adjacent Rhizones over 10 cm of core, usually <20 mL of total water was collected. Waters from Rhizone sampling were usually reserved for *Viking*-based pH and alkalinity measurements, *Oden*-based  $\text{NH}_4^+$  measurements, and shore-based metal and stable isotope analyses.

### Offshore interstitial water analyses

Four types of measurements on water samples were made during the offshore component of Expedition 302: salinity, pH, alkalinity aboard the *Vidar Viking*, and  $\text{NH}_4^+$  aboard the *Oden*. All other chemistry was analyzed onshore using preserved water samples and sediment samples.

With regard to the measurements made on the *Vidar Viking*, it is worth noting two complications. First, on most days, there was a  $10^\circ\text{C}$  temperature gradient from the lower bow end of the laboratory to the opposite upper stern end. The average temperature within the laboratory also varied from  $11^\circ$  to  $19^\circ\text{C}$ . Second, the laboratory, which was placed on the stern, experienced extreme vibrations, especially when ice was caught in the propellers. At times, an apt analogy for working conditions in terms of sound and motion was sitting on a freight train barreling through level crossings at 120 km/h.

Salinity ( $S$ ) to the nearest part per thousand was measured using a Krüss Optronic DR 301-95 digital refractometer. Approximately 1 mL of sample was placed onto the prism, the lid was closed, and the salinity (after calibration) was recorded. Further details are presented in the “Bremen Core Curation Van Handbook.” Multiple measurements of Arctic surface seawater consistently gave  $S = 34$  after temperature correction.

Alkalinity and pH were measured together using an electrode calibrated to known standards of 4.00 and 7.00 pH, and the “fast titration” method of Grasshoff (1983) was followed. A sample of 2.00 to 3.00 mL was pipetted into a 5.0 mL cup with a magnetic stir bar. The electrode was then inserted into the solution, the solution was stirred, and the pH was recorded. A burette was filled with 0.01M HCl. A small polytetrafluoroethylene (PTFE) microtube was attached to the burette at one end and the electrode to the other end so that acid could be slowly dispensed into the sample. While the solution was still being stirred, a titration was performed to a pH of ~3.8. The amount of acid added and the final pH value were recorded. Alkalinity was determined through equations outlined in the “Bremen Core Curation Van Handbook.” Multiple measurements of Arctic surface seawater gave a pH of  $7.8 \pm 0.1$  and an alkalinity of  $2.1 \pm 0.1$  mM.

Ammonium ( $\text{NH}_4^+$ ) concentrations were determined by the “Teflon tape gas separator method” (Hall and Aller, 1992). In general, this technique works as follows. An alkaline buffer comprising Na citrate dihydrate in a 10 mM NaOH solution is separated from a 1 mM HCl solution by a Teflon membrane. When samples are added to the buffer,  $\text{NH}_4^+$  ions in the sample are transformed to  $\text{NH}_3$ . Ammonia ( $\text{NH}_3$ ) then passes through the membrane, where it dissolves, causing a conductivity change. The change in conductivity can be calibrated to the amount of  $\text{NH}_4^+$  ion. During Expedition 302, 0.5 mL of sample was injected into the buffer solution. Each sample was analyzed twice, and the values were averaged. The estimated error in these measurements is  $\pm 5$   $\mu\text{M}$ .

### Onshore interstitial water analyses

Using analytical equipment housed in the Department of Geosciences, University of Bremen, some aliquots of IW samples were analyzed for a suite of dissolved species. These included major and trace elements by inductively coupled plasma–optical emission spectrometer (ICP-OES), chloride by titration, sulfate by ion chromatography, and phosphate by photometry. Deionized water used during these analyses was Milli-Q 18 M water.

Dissolved cations were analyzed using a PerkinElmer Optima 3300 R simultaneous ICP-OES ([www.geochemie.uni-bremen.de/koelling/icpoes.html](http://www.geochemie.uni-bremen.de/koelling/icpoes.html)). Most samples used for these analyses were those spiked aboard *Vidar Viking* with concentrated  $\text{HNO}_3$ . However, alkalinity splits were examined in some cases. In a first run, aliquots of samples were diluted 1:10 (or 1:5 for alkalinity splits) with deionized water and analyzed three times for B (249.772 nm), Ca (317.933 nm), Fe (259.939 nm), K (766.490 nm), Mg

(279.077 nm), Mn (259.372 nm), S (181.975 nm), Si (251.611 nm), and Sr (421.552 nm) using a cross-flow nebulizer. In a second run, aliquots of samples were diluted 1:20 (or 1:10 for alkalinity splits) with deionized water and analyzed three times for Al, Ba, Co, Cu, Ni, Pb, V, Y, Zn, and Zr using an ultrasonic nebulizer CETAC USN 5000AT. Concentrations of elements were determined by comparison to a curve defined by multiple dilutions of a multielement standard prepared from single-element standards with a 0.5M NaCl solution as a matrix background. Concentrations of all elements analyzed in the second run were at or near the detection limit, so they are not reported.

Chloride and bromide were collectively measured by titration with  $\text{AgNO}_3$ . Precisely 100 L of sample was added to 5 mL deionized water and then spiked with 100 L potassium chromate indicator solution. This was titrated with a 0.1M  $\text{AgNO}_3$  solution until the color changed from bright yellow to light orange. The titration was calibrated by 20 replicate analyses of International Association of Physical Sciences Organizations (IAPSO) standard, which gave an average sum for  $\text{Cl}^-$  and  $\text{Br}^-$  of 0.563 mM. All samples were analyzed three times; the precision of these replicates was consistently within 2 mM.

Sulfate was measured using an ion chromatography system comprising a Knauer autosampler 7500, a Thermo Separation Products pump, a 250 mm  $\times$  4 mm GA-1 anion column packed with 100 m PRP- $\times$ 100 beads, and a Knauer ultraviolet-visible light detector operating at 288 nm ([www.geochemie.uni-bremen.de/koelling/so4.html](http://www.geochemie.uni-bremen.de/koelling/so4.html)). The eluant used in this system was a 3 mM potassium hydrogen phthalate (KHP) solution adjusted to pH = 6.8 with KOH, with 5 mL/L of methanol added for sterilization. Samples were diluted 1:20 with deionized water. Concentrations were determined by comparison to IAPSO seawater, and dilutions of this standard were prepared using sulfate-free artificial seawater. Estimated errors in sulfate measurements were ~1 mM.

Dissolved phosphate was analyzed by the molybdenum blue method using a Merck portable photometer SQ118 (see [www.geochemie.uni-bremen.de/koelling/po4\\_fotom.html](http://www.geochemie.uni-bremen.de/koelling/po4_fotom.html)). To precisely a 1 mL sample in a microcuvette, 50 L of ammonium molybdate solution and 50 L of ascorbic acid solution were added. Samples were shaken and placed in the dark for 10 min. They were then analyzed at a wavelength of 820 nm. Concentrations were determined by comparison to a curve defined by seven dilutions of a phosphate standard.

In addition to the above measurements, aliquots that received zinc acetate were examined for precipitates. Samples with a white precipitate should indi-

cate the original presence of dissolved hydrogen sulfide; samples with a reddish orange precipitate should indicate the original presence of dissolved iron.

### Onshore sediment analyses

A suite of samples was taken for analyses of major element contents, minor element contents, carbonate content, organic carbon content, and mineralogical composition. The samples generally included one 10 cm<sup>3</sup> aliquot of sediment from available cores, all squeezecakes, and a few selected horizons of interest (e.g., rocks and nodules). A second suite of samples was also taken for analyses of carbonate content, organic carbon content, organic matter properties, and mineralogy. These samples generally came from available core catchers. Sediment samples were frozen, freeze-dried to remove water, and ground by hand with an agate mortar and pestle. Rock samples were air-dried, photographed, and cut to obtain small fragments. Many fragments were examined by scanning electron microscope (SEM) (see “[Supplementary Material](#)”); some fragments were also ground for compositional analyses. All preparation and analyses for the first suite of samples were performed at the Department of Geosciences, University of Bremen. The second set of samples was prepared and analyzed at Alfred Wegner Institute (AWI) (Germany), except for the mineralogy, which was conducted at University of Bremen.

Samples were analyzed for major and minor elements using a Spectro XEPOS portable energy dispersive polarization X-ray fluorescence analyzer, a system specifically designed for rapid analysis of marine sediment chemistry (e.g., Wien et al., in press). Approximately 5 g of dried and powdered sample was packed into a cuvette with a mylar foil bottom. Ten or eleven cuvettes of samples were then placed into an autosampler along with one or two cuvettes of three different standards to assess accuracy and precision. Results of 16 total replicates of U.S. Geological Survey MAG-1 standard, 6 total replicates of Bremen internal standard MAX, and 3 total replicates of Bremen internal standard CAMAX, are presented in Table T7. We note that the system has problems analyzing samples with high sulfur contents.

Sediment samples were analyzed for contents of organic carbon, carbonate, and sulfur using a LECO CS-200 IH carbon-sulfur analyzer at University of Bremen or a LECO CC-125 at AWI (see “[Organic geochemistry](#)”). Approximately 50 mg of dried, ground sample was weighed in a ceramic cup and heated in a furnace. The evolved CO<sub>2</sub> and SO<sub>2</sub> were then measured with a nondispersive infrared detector. A second aliquot of ~90 mg was weighed in a ce-

ramic cup, reacted with 12.5% HCl twice, washed with deionized water twice, and reanalyzed as above. The CO<sub>2</sub> measured in the second run was assumed to come from organic carbon. The analytical precision is about ±0.02% absolute.

Samples were analyzed for their mineralogical composition as described in “[X-ray diffraction](#)” in “[Lithostratigraphy](#).”

Several pieces of rocks, concretions, or nodules were examined using a Camscan CS 44 SEM equipped with a Phillips energy dispersive system (EDX-PV 98) to obtain semiquantitative elemental analyses. Samples were mounted on carbon-coated stubs and lightly coated with gold.

### Organic geochemistry

Total organic carbon (TOC) content was determined on bulk ground samples using a LECO CS-125 analyzer. The analytical precision is about ±0.02% absolute.

Rock-Eval pyrolysis was conducted on bulk sediment samples (with TOC content >0.3 wt%) to determine the amount of hydrocarbons already present in the sample (S1 peak in milligrams hydrocarbons per gram sediment), the amount of hydrocarbons generated by pyrolytic degradation of the kerogen during heating to 550°C (S2 peak in milligrams hydrocarbon per gram sediment), the amount of carbon dioxide generated during heating to 390°C (S3 peak in milligram carbon dioxide per gram sediment), and the temperature of maximum pyrolysis yield ( $T_{\max}$  value in degrees Celsius) (Espitalié et al., 1977; Peters, 1986). As further indicators for the composition of the organic matter, the Rock-Eval parameters hydrogen index (HI) and oxygen index (OI) values were used (cf. Tissot and Welte, 1984; Stein, 1991, and further references therein). HI corresponds to the quantity of pyrolyzable hydrocarbons per gram TOC (mg HC/g C), and OI corresponds to the quantity of carbon dioxide per gram TOC (mg CO<sub>2</sub>/g C). HI values <100 indicate a dominantly terrigenous (higher plant) source of organic matter, whereas HI values of 200–400 indicate the presence of major amount of aquatic algae (marine or freshwater) and/or microbial biomass.  $T_{\max}$  values <435°C are an indication of fresh immature organic matter, whereas  $T_{\max}$  values >435°C point to the presence of more mature and/or refractive organic matter.

### Microbiology

One finding of great significance from ODP was the discovery of microorganisms living in deeply buried marine sediments (see Parkes et al., 2000, for review).



To date, microorganisms have been observed in samples collected at depths as great as ~880 mbsf. Extrapolation of these data to total global ocean sediments suggests that the marine subsurface contains a significant fraction of the biomass on Earth (Whitman et al., 1998). However, the global coverage of sites examined for microorganisms is still quite sparse. Arctic sediments are completely unexplored with respect to microbiological parameters. Therefore, the results of this expedition will allow us to determine whether our current working models of global life in deeply buried marine sediments apply to this region as well. In addition to the total biomass, the structure, diversity, and function of subsurface microbial communities remain poorly understood.

### Core handling and sampling

In order to better evaluate microbiological data in the geochemical setting, microbiological samples were taken adjacent to whole-round samples collected for IW chemistry. All microbiological analyses will be conducted at shore-based laboratories. Therefore, it was imperative to collect clean samples and to prepare them properly for storage and transport. Because the samples were retrieved from a very stable sedimentary environment, the microorganisms are presumed to be sensitive to chemical and physical change, particularly oxygen, temperature, and pressure. Consequently, microbiological samples were taken on the *Vidar Viking* as soon as the core passed through the MSCL (~20 min after sectioning). It is essential to handle these sediment samples aseptically to prevent introduction of extraneous bacteria. As the sediments are predominantly anoxic, anaerobic handling methods must be used to prevent the introduction of oxygen. In addition, as the core liner is not sterile and the outer surface of the core is contaminated during drilling, subsamples for microbiological analyses were taken from the uncontaminated interior of the core (Smith et al., 2000). After the whole round was cut and removed, a sterile spatula was used to scrape a small section of the freshly exposed sediment surface. Sterile polypropylene syringes (3, 10, or 60 cm<sup>3</sup>) with the luer-lock end cut off were pushed into the core to collect subcores aseptically. The syringes containing the sediment subcore were then treated as follows depending on the intended downstream analysis.

### Nucleic acid analyses

Syringes with samples for deoxyribonucleic acid (DNA) analyses were sealed with parafilm on the exposed end and placed in a trilaminate foil bag (Schoelle) and heat-sealed. The samples were then

transferred to an ultra-low-temperature freezer (-57°C) for transport to shore-based laboratories. Nucleic acid analyses (e.g., small subunit ribosomal gene sequencing) will be performed in shore-based laboratories. These analyses will be used to determine the community structure of the microorganisms inhabiting the deep-buried marine sediments of the Lomonosov Ridge.

### Total cell counts

The most immediate method to visualize and quantify the deep microbial biosphere is total bacterial cell counts using the nucleic acid stain acridine orange. These counts have been made on a wide range of ODP (Parkes et al., 1994) and IODP sediment cores. In general, these counts have demonstrated an exponential decrease of microbial cells with depth below seafloor. Yet, minimum cell densities of 10<sup>4</sup>–10<sup>5</sup> cells/cm<sup>3</sup> have been consistently detected even in the deepest sediments. The method detects sediment layers of increased cell density that often coincide with particular geochemical conditions that are conducive to bacterial growth (Parkes et al., 2000). Subcores (1 cm<sup>3</sup>) collected in cutoff syringes were extruded into sterile polypropylene tubes containing filter-sterilized (0.2 µm) formalin in 3.5% NaCl. The tubes were stored at 4°C for transport to a shore-based laboratory. Microorganisms in the samples will be enumerated using epifluorescence microscopy after staining the DNA fluorochrome acridine orange (Fry et al., 1988).

### Biomarker analysis

Syringes with samples for DNA analyses were sealed with parafilm on the exposed end and placed in a trilaminate foil bag (Schoelle) and heat-sealed. The samples were then transferred to an ultra-low-temperature freezer (-57°C) for transport to shore-based laboratories. Biomarker analyses will be conducted in shore-based laboratories. These analyses will be used to determine the community structure of the subsurface microbial community.

### Cultivation techniques

Syringes with samples for cultivation experiments were placed in a plastic bag containing oxygen scrubber (Anaerocult) that was previously wetted. The bag was heat-sealed and then placed inside of a trilaminate bag (Schoelle) that was then heat-sealed. The bags were stored at 4°C for transport. This method of storage has been shown to maintain anaerobic conditions for months (Cragg et al., 1992). Attempts at cultivating microorganisms from these sediment samples will be conducted onshore.



## Paleomagnetism

Sediments recovered during Expedition 302 were sampled at BCR by the U-channel method for paleomagnetic and environmental magnetic studies. All sections were sampled except those that were obviously severely disturbed by drilling (e.g., flow-in or slurry).

The details of the U-channel sampling method are shown in Figure F10. The first step is to press or implant the U-channel into the core section (Fig. F10A). For lithologic Subunits 1/1 and 1/2, this implant was done by hand, whereas for Subunits 1/3, 1/4, and 1/5, a spatula was used to cut slots along the sides of the U-channel, and then the U-channel was driven into the core section with small mallets. Finally, for lithologic Subunit 1/6 and Units 2 and 3, the sections were marked, slots were cut using a cast-cutter saw, and the U-channel was driven into the slots using hand mallets.

Removal of the U-channel was achieved by a similar method that involved making a bottom cut using a range of cutting implements. The cutting implement used for the bottom cut depended on the stiffness of the material sampled. Cutters with a U cross-section were used for lithologic Subunits 1/1 and 1/2, whereas a spring-wire cutter was used for Subunit 1/3 through Unit 3. Most U-channels were lifted directly out of the core sections after the bottom cut was made. U-channels from wet, sticky, or crumbly lithologies were removed by inserting the core sections into an open-ended D-tube with a slot cut down the middle of the upper surface. The D-tube containing the core section was turned upside down (Fig. F10B), and the U-channel was pulled from the section using gravity as an aid (Fig. F10C).

After the U-channel was removed, residue was cleaned from all surfaces and saved for magnetic extraction studies. The U-channel cap was snapped on, and the ends were taped shut. The U-channels were then stored in D-tubes.

Magnetostratigraphic studies of the U-channels were done at the University of Rhode Island (URI; USA) using a 2G Enterprises 755R pass-through magnetometer and at CEREGE (France) using a 2G Enterprises 760 pass-through direct-current superconducting quantum interference devices (DC-SQUID) magnetometer. DC-SQUID sensors measure currents induced in superconducting coils (three total: two for transverse and one for axial moment measurement). The primary difference between the two systems is sample diameter, where URI's has a smaller diameter limit than CEREGE's but increased sensitivity. Intercalibration studies will be done to ensure the comparability of the data.

Measurements were made of the initial natural remanent magnetization (NRM) and the NRM remaining after a series of AF demagnetization steps (maximum peak AF field of 40–55.0 mT).

## References

- Akiba, F., 1986. Middle Miocene to Quaternary diatom biostratigraphy in the Nankai Trough and Japan Trench, and modified lower Miocene through Quaternary diatom zones for middle-to-high latitudes of the North Pacific. *In* Kagami, H., Karig, D.E., Coulbourn, W.T., et al., *Init. Repts. DSDP*, 87: Washington (U.S. Govt. Printing Office), 393–481.
- Amigo, A.E., 1999. Miocene silicoflagellate stratigraphy: Iceland and Rockall Plateaus. *In* Raymo, M.E., Jansen, E., Blum, P., and Herbert, T.D. (Eds.), 1999. *Proc. ODP, Sci. Results*, 162: College Station, TX (Ocean Drilling Program), 63–81. [HTML]
- Andersen, E.S., Dokken, T.M., Elverhøi, A., Solheim, A., and Fossen, I., 1996. Late Quaternary sedimentation and glacial history of the western Svalbard continental margin. *Mar. Geol.*, 133:123–156. doi:10.1016/0025-3227(96)00022-9
- ASTM International, 2005. Standard test methods for laboratory determination of water (moisture) content of soil and rock by mass. (Standard D2216-05). *In Annual Book of ASTM Standards* (Vol. 04.08): *Soil and Rock* (I): West Conshohocken, PA (Am. Soc. Testing and Mater.).
- Berggren, W.A., Kent, D.V., Swisher, C.C., III, and Aubry, M.-P., 1995. A revised Cenozoic geochronology and chronostratigraphy. *In* Berggren, W.A., Kent, D.V., Aubry, M.-P., and Hardenbol, J. (Eds.), *Geochronology, Time Scales and Global Stratigraphic Correlation*. Spec. Publ.—SEPM (Soc. Sediment. Geol.), 54:129–212.
- Bjørklund, K.R., 1976. Radiolaria from the Norwegian Sea, Leg 38 of the Deep Sea Drilling Project. *In* Talwani, M., Udintsev, G., et al., *Init. Repts. DSDP*, 38: Washington (U.S. Govt. Printing Office), 1101–1168.
- Blatt, H., Middleton, G.V., and Murray, R., 1980. *Origin of Sedimentary Rocks* (2nd ed.): Englewood Cliffs, NJ (Prentice-Hall).
- Blum, P., 1997. Physical properties handbook: a guide to the shipboard measurement of physical properties of deep-sea cores. *ODP Tech. Note*, 26 [Online]. Available from World Wide Web: <<http://www-odp.tamu.edu/publications/tnotes/tn26/INDEX.HTM>>.
- Boyce, R.E., 1976. Definitions and laboratory techniques of compressional sound velocity parameters and wet-water content, wet-bulk density, and porosity parameters by gravimetric and gamma-ray attenuation techniques. *In* Schlanger, S.O., Jackson, E.D., et al., *Init. Repts. DSDP*, 33: Washington (U.S. Govt. Printing Office), 931–958.
- Brouwers, E.M., Jørgensen, N.O., and Cronin, T.M., 1991. Climatic significance of the ostracode fauna from the Pliocene Kap København Formation, north Greenland. *Micropaleontology*, 37:245–267.
- Bukry, D., 1984. Paleogene paleoceanography of the Arctic Ocean is constrained by the middle or late Eocene age

- of USGS Core FI-422: evidence from silicoflagellates. *Geology*, 12:199–201. doi:10.1130/0091-7613(1984)12<199:PPOTAO>2.0.CO;2
- Cande, S.C., and Kent, D.V., 1995. Revised calibration of the geomagnetic polarity timescale for the Late Cretaceous and Cenozoic. *J. Geophys. Res.*, 100:6093–6095. doi:10.1029/94JB03098
- Coles, G., and Whatley, R., 1989. New Paleogene to Miocene genera and species of Ostracoda from DSDP Sites in the North Atlantic. *Rev. Esp. Micropaleontol.*, 21:81–124.
- Cragg, B.A., Bale, S.J., and Parkes, R.J., 1992. A novel method for the transport and long-term storage of cultures and samples in an anaerobic atmosphere. *Letts. Appl. Microbiol.*, 15:125–128.
- Cronin, T.M., 1991. Late Neogene marine Ostracoda from Tjörnnes, Iceland. *J. Paleontol.*, 65:767–794.
- Cronin, T.M., Holtz, T.R., and Whatley, R.P., 1994. Quaternary paleoceanography of the deep Arctic Ocean based on quantitative analysis of Ostracoda. *Mar. Geol.*, 19:305–332. doi:10.1016/0025-3227(94)90188-0
- Cronin, T.M., Holtz, T.R., Jr., Stein, R., Spielhagen, R., Fütterer, D., and Wollenberg, J., 1995. Late Quaternary paleoceanography of the Eurasian Basin, Arctic Ocean. *Paleoceanography*, 10:259–281. doi:10.1029/94PA03149
- Cronin, T.M., and Whatley, R., 1996. Ostracoda from Sites 910 and 911. In Thiede, J., Myhre, A.M., Firth, J.V., Johnson, G.L., and Ruddiman, W.F. (Eds.), *Proc. ODP, Sci. Results*, 151: College Station, TX (Ocean Drilling Program), 197–201.
- Curry, W.B., Shackleton, N.J., Richter, C., et al., 1995. *Proc. ODP, Init. Repts.*, 154: College Station, TX (Ocean Drilling Program).
- Dell’Agnese, D., and Clark, D.L., 1994. Siliceous microfossils from the warm Late Cretaceous and early Cenozoic Arctic Ocean. *J. Paleontol.*, 68:31–46.
- D’Hondt, S.L., Jørgensen, B.B., Miller, D.J., et al., 2003. *Proc. ODP, Init. Repts.*, 201 [CD-ROM]. Available from: Ocean Drilling Program, Texas A&M University, College Station TX 77845-9547, USA. [HTML]
- Diepenbroek, M., Grobe, H., Reinke, M., Schlitzer, R., and Sieger, R., 1999. Data management of proxy parameters with PANGAEA. In Fischer, G., and Wefer, G. (Eds.), *Use of Proxies in Paleoceanography—Examples from the South Atlantic*: Heidelberg (Springer), 715–727.
- Diepenbroek, M., Grobe, H., Reinke, M., Schindler, U., Schlitzer, R., Sieger, R., and Wefer, G., 2002. PANGAEA—an information system for environmental sciences. *Comp. Geosci.*, 28:1201–1210. doi:10.1016/S0098-3004(02)00039-0
- Doyle, P.S., and Riedel, W.R., 1979. Cretaceous to Neogene ichthyoliths in a giant piston core from the central North Pacific. *Micropaleontology*, 25:337–364.
- Dzinoridze, R.N., Jousé, A.P., Koroleva-Golikova, G.S., Kozlova, G.E., Nagaeva, G.S., Petrushevskaya, M.G., and Strelnikova, N.I., 1978. Diatom and radiolarian Cenozoic stratigraphy, Norwegian Basin; DSDP Leg 38. In Talwani, M., Udintsev, G., et al., *Init. Repts. DSDP*, 38, 39, 40, 41 (Suppl.): Washington (U.S. Govt. Printing Office), 289–427.
- Eldrett, J.S., Harding, I.C., Firth, J.V., and Roberts, A.P., 2004. Magnetostratigraphic calibration of Eocene–Oligocene dinoflagellate cyst biostratigraphy from the Norwegian–Greenland Sea. *Mar. Geol.*, 204:91–127. doi:10.1016/S0025-3227(03)00357-8
- Ellis, D.V., 1987. *Well Logging for Earth Scientists*: New York (Elsevier).
- Espitalié, J., Laporte, J.L., Madec, M., Marquis, F., Leplat, P., Paulet, J., and Boutefeu, A., 1977. Méthode rapide de caractérisation des roches mères, de leur potentiel pétrolier et de leur degré d’évolution. *Rev. Inst. Fr. Pet.*, 32:23–42.
- Evans, J.R., and Kaminski, M., 1998. Pliocene and Pleistocene chronostratigraphy and paleoenvironment of the central Arctic Ocean, using deep water agglutinated foraminifera. *Micropaleontology*, 44:109–130.
- Fenner, J., 1985. Late Cretaceous to Oligocene planktic diatoms. In Bolli, H.M., Saunders, J.B., and Perch-Nielsen, K. (Eds.), *Plankton Stratigraphy*: Cambridge (Cambridge Univ. Press), 713–762.
- Feyling-Hanssen, R., 1990. A remarkable foraminiferal assemblage from the Quaternary of northeast Greenland. *Bull. Geol. Soc. Den.*, 38:101–107.
- Firth, J.V., 1996. Upper middle Eocene to Oligocene dinoflagellate biostratigraphy and assemblage variations in Hole 913B, Greenland Sea. In Thiede, J., Myhre, A.M., Firth, J.V., Johnson, G.L., and Ruddiman, W.F. (Eds.), *Proc. ODP, Sci. Results*, 151: College Station, TX (Ocean Drilling Program), 203–242.
- Fry, J.C., 1988. Determination of biomass. In Austin, B. (Ed.), *Methods in Aquatic Bacteriology*: Chichester (Wiley), 27–72.
- Gieskes, J.M., Gamo, T., and Brumsack, H., 1991. Chemical methods for interstitial water analysis aboard JOIDES Resolution. *ODP Tech. Note*, 15 [Online]. Available from World Wide Web: <[http://www-odp.tamu.edu/publications/tnotes/tn15/f\\_chem1.htm](http://www-odp.tamu.edu/publications/tnotes/tn15/f_chem1.htm)>.
- Gleason, J.D., Moore, T.C., Johnson, T.M., Rea, D.K., Blum, J.D., Owen, R.M., Pares, J., and Hovan, S.A., 2004. Age calibration of a piston Core EW9709-07 (equatorial central Pacific) using fish teeth Sr isotope stratigraphy: new tools for quantifying Neogene dust sources and sinks in the marine record. *Palaeogeogr., Palaeoclimatol., Palaeoecol.*, 212:355–366. doi:10.1016/j.palaeo.2004.07.005
- Goldberg, D., 1997. The role of downhole measurements in marine geology and geophysics. *Rev. Geophys.*, 35:315–342. doi:10.1029/97RG00221
- Goll, R.M., and Bjørklund, K.R., 1989. A new radiolarian biostratigraphy for the Neogene of the Norwegian Sea: ODP Leg 104. In Eldholm, O., Thiede, J., Taylor, E., et al., *Proc. ODP, Sci. Results*, 104: College Station, TX (Ocean Drilling Program), 697–737.
- Gradstein, F.M., Kaminski, M.A., Berggren, W.A., Kristiansen, I.L., and D’Iorio, M.A., 1994. Cenozoic biostratigraphy of the North Sea and Labrador Shelf. *Micropaleontology*, 40(Suppl.):1–152.
- Grasshoff, K., Ehrhardt, M., and Kemling, K., 1983. *The Methods of Seawater Analysis*: Weinheim, F.R.G. (Verlag Chemie).

- Hagelberg, T., Shackleton, N., Pisias, N., and Shipboard Scientific Party, 1992. Development of composite depth sections for Sites 844 through 854. *In* Mayer, L., Pisias, N., Janecek, T., et al., *Proc. ODP, Init. Repts.*, 138 (Pt. 1): College Station, TX (Ocean Drilling Program), 79–85.
- Hagelberg, T.K., Pisias, N.G., Shackleton, N.J., Mix, A.C., and Harris, S., 1995. Refinement of a high-resolution, continuous sedimentary section for studying equatorial Pacific Ocean paleoceanography, Leg 138. *In* Pisias, N.G., Mayer, L.A., Janecek, T.R., Palmer-Julson, A., and van Andel, T.H. (Eds.), *Proc. ODP, Sci Results*, 138: College Station, TX (Ocean Drilling Program), 31–46.
- Hall, P.O.J., and Aller, R.C., 1992. Rapid small-volume flow injection analysis for CO<sub>2</sub> and NH<sub>4</sub> in marine sediments. *Limnol. Oceanogr.*, 35:1113–1115.
- Hansbo, S., 1957. A new approach to the determination of the shear strength of clay by the fall-cone test. *Swed. Geotech. Inst. Publ.*, 14.
- Head, M.J., and Norris, G., 1989. Palynology and dinocyst stratigraphy of the Eocene and Oligocene in ODP Leg 105, Hole 647A, Labrador Sea. *In* Srivastava, S.P., Arthur, M.A., Clement, B., et al., *Proc. ODP, Sci. Results*, 105: College Station, TX (Ocean Drilling Program), 515–550.
- Holtz, R.D., and Kovacs, W.D., 1981. *An Introduction to Geotechnical Engineering*: Englewood Cliffs, NJ (Prentice-Hall).
- Ishman, S.E., Polyak, L., and Poore, R.Z. 1996. Expanded record of Quaternary oceanographic change: Amerasian Arctic Ocean. *Geology*, 24:139–142. doi:10.1130/0091-7613(1996)024<0139:EROQOC>2.3.CO;2
- Jansen, E., Raymo, M.E., Blum, P., et al., 1996. *Proc. ODP, Init. Repts.*, 162: College Station, TX (Ocean Drilling Program).
- Kamikuri, S., Nishi, H., Motoyama, I., and Saito, S., 2004. Middle Miocene to Pleistocene radiolarian biostratigraphy in the northwest Pacific Ocean, ODP Leg 186. *Isl. Arc*, 13:191–226. doi:10.1111/j.1440-1738.2003.00421.x
- Kaminski, M.A., and Austin, W.E.N., 1999. Oligocene deep-water agglutinated foraminifera at Site 985, Norwegian Basin, southern Norwegian Sea. *In* Raymo, M.E., Jansen, E., Blum, P., and Herbert, T.D. (Eds.), 1999. *Proc. ODP, Sci. Results*, 162: College Station, TX (Ocean Drilling Program), 169–177. [HTML]
- Kaminski, M.A., Gradstein, F.M., Goll, R.M., and Greig, D., 1990. Biostratigraphy and paleoecology of deep-water agglutinated foraminifera at ODP Site 643, Norwegian-Greenland Sea. *In* Hemleben, C., Kaminski, M.A., Kuhnt, W., and Scott, D. (Eds.), *Paleoecology, Biostratigraphy, Paleoceanography and Taxonomy of Agglutinated Foraminifera*. NATO ASI Ser. C, 237:345–386.
- Keen, M., 1978. The Tertiary–Palaeogene. *In* Bate, R.H., and Robinson, E. (Eds.), *A Stratigraphic Index of British Ostracoda*. *Geol. J., Spec. Issue*, 8:385–450.
- Knudsen, K.L., and Asbjørnsdottir, L., 1991. Plio–Pleistocene foraminiferal stratigraphy and correlation in the central North Sea. *Mar. Geol.*, 101:113–124. doi:10.1016/0025-3227(91)90066-D
- Koç, N., and Scherer, R.P., 1996. Neogene diatom biostratigraphy of the Iceland Sea Site 907. *In* Thiede, J., Myhre, A.M., Firth, J.V., Johnson, G.L., and Ruddiman, W.F. (Eds.), *Proc. ODP, Sci. Results*, 151: College Station, TX (Ocean Drilling Program), 61–74.
- Kvenvolden, K.A., and McDonald, T.J., 1986. Organic geochemistry on the JOIDES Resolution—an assay. *ODP Tech. Note*, 6.
- Ling, H.Y., 1985. Early Paleogene silicoflagellates and ebridians from the Arctic Ocean. *Trans. Proc. Paleontol. Soc. Jpn.*, 138:79–93.
- Locker, S., 1996. Cenozoic siliceous flagellates from the Fram Strait and the East Greenland margin: biostratigraphic and paleoceanographic results. *In* Thiede, J., Myhre, A.M., Firth, J.V., Johnson, G.L., and Ruddiman, W.F. (Eds.), *Proc. ODP, Sci. Results*, 151: College Station, TX (Ocean Drilling Program), 101–124.
- Lovell, M.A., Harvey, P.K., Brewer, T.S., Williams, C., Jackson, P.D., and Williamson, G., 1998. Application of FMS images in the Ocean Drilling Program: an overview. *In* Cramp, A., MacLeod, C.J., Lee, S.V., and Jones, E.J.W. (Eds.), *Geological Evolution of Ocean Basins: Results from the Ocean Drilling Program*. *Geol. Soc. Spec. Publ.*, 131:287–303.
- Lyle, M., Koizumi, I., Richter, C., et al., 1997. *Proc. ODP, Init. Repts.*, 167: College Station, TX (Ocean Drilling Program). [HTML]
- Malz, H., 1989. Cenozoic ostracodes of the Vøring Plateau (ODP Leg 104, Sites 642, 643, and 644). *In* Eldholm, O., Thiede, J., Taylor, E., et al., *Proc. ODP, Sci. Results*, 104: College Station, TX (Ocean Drilling Program), 769–775.
- Martini, E., 1971. Standard Tertiary and Quaternary calcareous nannoplankton zonation. *In* Farinacci, A. (Ed.), *Proc. 2nd Int. Conf. Planktonic Microfossils Roma*: Rome (Ed. Tecnosci.), 2:739–785.
- McNeil, D.H., 1997. New foraminifera from the Upper Cretaceous and Cenozoic of the Beaufort-MacKenzie Basin of Arctic Canada. *Spec. Publ.—Cushman Found. Foraminiferal Res.*, 35:1–95.
- Moran, K., 1997. Elastic property corrections applied to Leg 154 sediment, Ceara Rise. *In* Shackleton, N.J., Curry, W.B., Richter, C., and Bralower, T.J. (Eds.), *Proc. ODP, Sci. Results*, 154: College Station, TX (Ocean Drilling Program), 151–155. [PDF]
- Munsell Color Company, Inc., 1971. *Munsell Soil Color Charts*: Baltimore, MD (Munsell).
- Murray, R.W., Miller, D.J., and Kryc, K.A., 2000. Analysis of major and trace elements in rocks, sediments, and interstitial waters by inductively coupled plasma–atomic emission spectrometry (ICP–AES). *ODP Tech. Note*, 29 [Online]. Available from World Wide Web: <<http://www-odp.tamu.edu/publications/tnotes/tn29/INDEX.HTM>>.
- Nagy, J., Kaminski, M.A., Gradstein, F.M., and Johnson, K., 2004. Quantitative foraminiferal and palynomorph biostratigraphy of the Paleogene in the southwestern Barents Sea. *In* Bubik, M., and Kaminski, M.A. (Eds.), *Proc. 6th Int. Workshop Agglutinated Foraminifera*. Grzybowski Found. *Spec. Publ.*, 8:359–379.
- Nagy, J., Kaminski, M.A., Kuhnt, W., and Bremer, M.A., 2000. Agglutinated foraminifera from neritic to bathyal facies in the Palaeogene of Spitsbergen and the Barents



- Sea. In Hart, M.B., Kaminski, M.A., and Smart, C.W. (Eds.), *Proc. 5th Int. Workshop Agglutinated Foraminifera*. Grzybowski Found. Spec. Publ., 7:333–361.
- Norris, R.D., Kroon, D., Klaus, A., et al., 1998. *Proc. ODP, Init. Repts.*, 171B: College Station, TX (Ocean Drilling Program). [HTML]
- Oertli, H.J. (Ed.), 1985. *Atlas des Ostracodes de France*. Mem. Bull. Cent. Rech. Explor.-Prod. Elf-Aquitaine, 9.
- Osterman, L.E., 1996. Pliocene and Quaternary benthic foraminifers from Site 910, Yermak Plateau. In Thiede, J., Myhre, A.M., Firth, J.V., Johnson, G.L., and Ruddiman, W.F. (Eds.), *Proc. ODP, Sci. Results*, 151: College Station, TX (Ocean Drilling Program), 187–195.
- Osterman, L.E., and Spiegler, D., 1996. Agglutinated benthic foraminiferal biostratigraphy of Sites 909 and 913, northern North Atlantic. In Thiede, J., Myhre, A.M., Firth, J.V., Johnson, G.L., and Ruddiman, W.F. (Eds.), *Proc. ODP, Sci. Results*, 151: College Station, TX (Ocean Drilling Program), 169–185.
- Osterman, L.E., and Qvale, G., 1989. Benthic foraminifers from the Vøring Plateau (ODP Leg 104). In Eldholm, O., Thiede, J., Taylor, E., et al., *Proc. ODP, Sci. Results*, 104: College Station, TX (Ocean Drilling Program), 745–768.
- Padman, L., and Erofeeva, S., 2004. A Barotropic inverse tidal model for the Arctic Ocean. *Geophys. Res. Lett.*, 31:L02303. doi:10.1029/2003GL019003
- Pälike, H., Moore, T., Backman, J., Raffi, I., Lanci, L., Parés, J.M., and Janecek, T., 2005. Integrated stratigraphic correlation and improved composite depth scales for ODP Sites 1218 and 1219. In Wilson, P.A., Lyle, M., and Firth, J.V. (Eds.), *Proc. ODP, Sci. Results*, 199 [Online]. Available from World Wide Web: <[http://www-odp.tamu.edu/publications/199\\_SR/213/213.htm](http://www-odp.tamu.edu/publications/199_SR/213/213.htm)>.
- Parkes, R.J., Cragg, B.A., Bale, S.J., Getliff, J.M., Goodman, K., Rochelle, P.A., Fry, J.C., Weightman, A.J., and Harvey, S.M., 1994. Deep bacterial biosphere in Pacific Ocean sediments. *Nature (London, U. K.)*, 371:410–413. doi:10.1038/371410a0
- Parkes, R.J., Cragg, B.A., and Wellsbury, P., 2000. Recent studies on bacterial populations and processes in marine sediments: a review. *Hydrogeol. Rev.*, 8:11–28.
- Penney, D.N., 1990. Quaternary ostracod chronology of central North Sea: the record from BH 81/29. *CFS, Cour. Forschungsinst. Senckenberg*, 123:97–109.
- Penney, D.N., 1993. Late Pliocene to early Pleistocene ostracod stratigraphy and palaeoclimate of the Lodin Elv and Kap København Formation, East Greenland. *Palaeogeogr., Palaeoclimatol., Palaeoecol.*, 101:49–66. doi:10.1016/0031-0182(93)90151-8
- Perch-Nielsen, K., 1985a. Cenozoic calcareous nannofossils. In Bolli, H.M., Saunders, J.B., and Perch-Nielsen, K. (Eds.), *Plankton Stratigraphy*: Cambridge (Cambridge Univ. Press), 427–554.
- Perch-Nielsen, K., 1985b. Silicoflagellates. In Bolli, H.M., Saunders, J.B., and Perch-Nielsen, K. (Eds.), *Plankton Stratigraphy*: Cambridge (Cambridge Univ. Press), 811–846.
- Peters, K.E., 1986. Guidelines for evaluating petroleum source rock using programmed pyrolysis. *AAPG Bull.*, 70:318–329.
- Petschick, R., Kuhn, G., and Gingele, F., 1996. Clay mineral distribution in surface sediments of the South Atlantic: sources, transport, and relation to oceanography. *Mar. Geol.*, 130:203–229. doi:10.1016/0025-3227(95)00148-4
- Podobina, V.M., 1998. *Paleogene Foraminifera and Biostratigraphy of Western Siberia*: Tomsk, Russia (Sci. Tech. Literature Publ.).
- Polyak, L., Curry, W.B., Darby, D.A., Bischof, J., and Cronin, T.M., 2004. Contrasting glacial/interglacial regimes in the western Arctic Ocean as exemplified by a sedimentary record from the Mendeleev Ridge. *Palaeogeogr., Palaeoclimatol., Palaeoecol.*, 203:73–93. doi:10.1016/S0031-0182(03)00661-8
- Repenning, C.A., Brouwers, E.M., Carter, L.D., Marincovitich, L., Jr., and Ager, T.A., 1987. The Beringian ancestry of *Phenacomys* (Rodentia: Cricetidae) and the beginning of the modern Arctic Ocean borderland biota. *U.S. Geol. Surv. Bull.*, 1687:1–28.
- Rider, M.H., 1996. *The Geological Interpretation of Well Logs* (2nd ed.): Caithness (Whittles Publishing).
- Riding, J.R., and Kyffin-Hughes, J.E., 2004. A review of the laboratory preparation of palynomorphs with a description of an effective non-acid technique. *Rev. Bras. Paleontol.*, 7:13–44.
- Ruddiman, W.F., Cameron, D., and Clement, B.M., 1987. Sediment disturbance and correlation of offset holes drilled with the hydraulic piston corer: Leg 94. In Ruddiman, W.F., Kidd, R.B., Thomas, E., et al., *Init. Repts. DSDP, 94 (Pt. 2)*: Washington (U.S. Govt. Printing Office), 615–634.
- Scherer, R.P., and Koç, N., 1996. Late Paleogene diatom biostratigraphy and paleoenvironments of the northern Norwegian-Greenland Sea. In Thiede, J., Myhre, A.M., Firth, J.V., Johnson, G.L., and Ruddiman, W.F. (Eds.), *Proc. ODP, Sci. Results*, 151: College Station, TX (Ocean Drilling Program), 75–99.
- Schlumberger, 1989. *Log Interpretation Principles/Applications*: Houston (Schlumberger Educ. Services), SMP-7017.
- Schlumberger, 1994. *IPL Integrated Porosity Lithology* (Schlumberger Wireline and Testing), SMP-9270.
- Schrader, H.-J., and Fenner, J., 1976. Norwegian Sea Cenozoic diatom biostratigraphy and taxonomy. In Talwani, M., Udintsev, G., et al., *Init. Repts. DSDP, 38*: Washington (U.S. Govt. Printing Office), 921–1099.
- Schröder-Adams, C.J., and McNeil, D.H., 1994. Oligocene to Miocene agglutinated foraminifera in deltaic and deep-water facies of the Beaufort-MacKenzie Basin. *Geol. Surv. Can. Bull.* 477:1–67.
- Scott, D.B., Mudie, P.J., Baki, V., MacKinnon, K.D., and Cole, F.E., 1989. Biostratigraphy and late Cenozoic paleoceanography of the Arctic Ocean: foraminiferal, lithostratigraphic, and isotopic evidence. *Geol. Soc. Am. Bull.*, 101:260–277. doi:10.1130/0016-7606(1989)101<0260:BALCPO>2.3.CO;2
- Seeberg-Elverfeldt, J., Schlüter, M., Feseker, T., and Kölling, M., submitted. A Rhizon in situ sampler (RISS) for pore water sampling from aquatic sediments. *Limnol. Oceanogr.*



- Serra, O., 1984. *Fundamentals of Well-Log Interpretation* (Vol. 1): *The Acquisition of Logging Data*. Dev. Pet. Sci., 15A: Amsterdam (Elsevier).
- Serra, O., 1986. *Fundamentals of Well-Log Interpretation* (Vol. 2): *The Interpretation of Logging Data*. Dev. Pet. Sci., 15B: Amsterdam (Elsevier).
- Shipboard Scientific Party, 1987. Explanatory notes: ODP Leg 105, Baffin Bay and Labrador Sea. In Srivastava, S.P., Arthur, M., et al., *Proc. ODP, Init. Repts.*, 105: College Station, TX (Ocean Drilling Program), 21–42.
- Shipboard Scientific Party, 1995. Explanatory notes. In Myhre, A.M., Thiede, J., Firth, J.V., et al., *Proc. ODP, Init. Repts.*, 151: College Station, TX (Ocean Drilling Program), 27–45.
- Shipboard Scientific Party, 2002. Leg 199 summary. In Lyle, M., Wilson, P.A., Janecek, T.R., et al., *Proc. ODP, Init. Repts.*, 199 [Online]. Available from World Wide Web: [http://www-odp.tamu.edu/publications/199\\_IR/chap\\_01/chap\\_01.htm](http://www-odp.tamu.edu/publications/199_IR/chap_01/chap_01.htm).
- Shipboard Scientific Party, 2003. Leg 202 summary. In Mix, A.C., Tiedemann, R., Blum, P., et al., *Proc. ODP, Init. Repts.*, 202 [Online]. Available from World Wide Web: [http://www-odp.tamu.edu/publications/202\\_IR/chap\\_01/chap\\_01.htm](http://www-odp.tamu.edu/publications/202_IR/chap_01/chap_01.htm).
- Siddiqui, Q.A., 1988. The Iperk Sequence (Plio–Pleistocene) and its ostracod assemblages in the eastern Beaufort Sea. In Hannai, T., Ikeya, N., and Ishizaki, K. (Eds.), *Evolutionary Biology of Ostracoda: its Fundamentals and Applications*. Dev. Palaeontol. Stratigr., 11:533–540.
- Smith, D.C., Spivack, A.J., Fisk, M.R., Haveman, S.A., and Staudigel, H., 2000. Tracer-based estimates of drilling-induced microbial contamination of deep sea crust. *Geomicrobiol. J.*, 17:207–219. doi:10.1080/01490450050121170
- Stein, R., 1991. Accumulation of organic carbon in marine sediments: results from the Deep Sea Drilling Project/Ocean Drilling Program (DSDP/ODP). In Battacharji, S., Friedman, G.M., Neugebauer, H.J., and Seilacher, A. (Eds.), *Lecture Notes in Earth Sciences* (Vol. 34): Berlin (Springer-Verlag), 217.
- Spiegler, D., 1996. Planktonic foraminifer Cenozoic biostratigraphy of the Arctic Ocean, Fram Strait (Sites 908–909), Yermak Plateau (Sites 910–912), and East Greenland margin (Site 913). In Thiede, J., Myhre, A.M., Firth, J.V., Johnson, G.L., and Ruddiman, W.F. (Eds.), *Proc. ODP, Sci. Results*, 151: College Station, TX (Ocean Drilling Program), 153–167.
- Spiegler, D., and Jansen, E., 1989. Planktonic foraminifer biostratigraphy of Norwegian Sea sediments: ODP Leg 104. In Eldholm, O., Thiede, J., Taylor, E., et al., *Proc. ODP, Sci. Results*, 104: College Station, TX (Ocean Drilling Program), 681–696.
- Szczuchura, J., 1971. Paleocene ostracoda from Nugssuaq, West Greenland. *Bull.—Groenl. Geol. Unders.*, 165(193):1–42.
- Tissot, B.P., and Welte, D.H., 1984. *Petroleum Formation and Occurrence*: Heidelberg (Springer-Verlag).
- Vogt, C., 1997. Regional and temporal variations of mineral assemblages in Arctic Ocean sediments as climatic indicator during glacial/interglacial changes [Ph.D. thesis]. Alfred Wegener Institute Bremerhaven.
- Vogt, C., Knies, J., Spielhagen, R.F., and Stein, R., 2001. Detailed mineralogical evidence for two nearly identical glacial/deglacial cycles and Atlantic water advection to the Arctic Ocean during the last 90,000 years. *Global Planet. Change*, 31:23–44. doi:10.1016/S0921-8181(01)00111-4
- Von Herzen, R.P., and Maxwell, A.E., 1959. The measurement of thermal conductivity of deep-sea sediments by a needle-probe method. *J. Geophys. Res.*, 64:1557–1563.
- Weaver, P.P.E., and Clement, B.M., 1986. Synchronicity of Pliocene planktonic foraminiferal datums in the North Atlantic. *Mar. Micropaleontol.*, 10:295–307. doi:10.1016/0377-8398(86)90033-2
- Whatley, R., and Coles, G., 1987. The late Miocene to Quaternary Ostracoda of Leg 94, Deep Sea Drilling Project. *Rev. Esp. Micropaleontol.*, 19:33–97.
- Whitman, W.B., Coleman, D.C., and Wiebe, W.J., 1998. Prokaryotes: the unseen majority. *Proc. Nat. Acad. Sci. U.S.A.*, 95:6578–6583. doi:10.1073/pnas.95.12.6578
- Wien, K., Wissman, D., Kolling, M., and Schulz, H.D., 2005. Fast application of X-ray fluorescence spectrometry aboard ship: how good is the portable Spectro Xepos analyser? *Geo-Mar. Lett.*, 25:248–264. doi:10.1007/s00367-004-0206-x
- Williams, G.L., Brinkhuis, H., Pearce, M.A., Fensome, R.A., and Weegink, J.W., 2004. Southern Ocean and global dinoflagellate cyst events compared: index events for the Late Cretaceous–Neogene. In Exxon, N.F., Kennett, J.P., and Malone, M. (Eds.), *Proc. ODP, Sci. Results*, 189 [Online]. Available from World Wide Web: [http://www-odp.tamu.edu/publications/189\\_SR/107/107.htm](http://www-odp.tamu.edu/publications/189_SR/107/107.htm).
- Williams, G.L., Lentin, J.K., and Fensome, R.A., 1998. *The Lentin and Williams Index of Fossil Dinoflagellate Cysts* (1998 ed.). Am. Assoc. Stratigr. Palynol., Contrib. Ser., Vol. 34.
- Williams, G.L., and Manum, S.B., 1999. Oligocene–early Miocene dinocyst stratigraphy of Hole 985A (Norwegian Sea). In Raymo, M.E., Jansen, E., Blum, P., and Herbert, T.D. (Eds.), 1999. *Proc. ODP, Sci. Results*, 162: College Station, TX (Ocean Drilling Program), 99–109. [HTML]
- Yanagisawa, Y., and Akiba, F., 1998. Refined Neogene diatom biostratigraphy for the northwest Pacific around Japan, with an introduction of code numbers for selected diatom biohorizons. *J. Geol. Soc. Jpn.*, 104:395–414.
- Zreiek, D.A., Ladd, C.C., and Germaine, J.T., 1995. A new fall cone device for measuring the undrained strength of very weak cohesive soils. *Geotech. Test. J.*, 18(4):472–482.

**Publication:** 7 March 2006  
**MS 302-103**

Figure F1. Example of core section engraving and labeling.

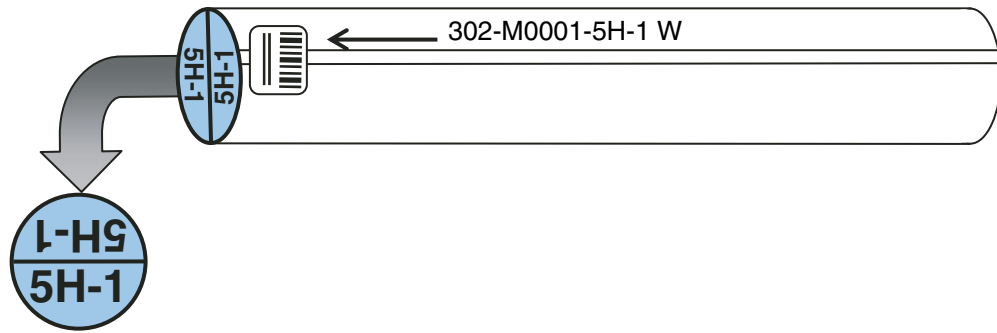


**Figure F2.** Keys to symbols used in the Graphic Lithology column in the core descriptions (modified from Shipboard Scientific Party, 1995).

**Biogenic sediments**

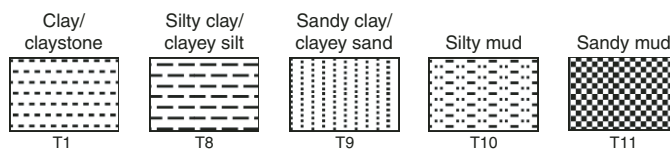
Siliceous

Siliceous  
ooze

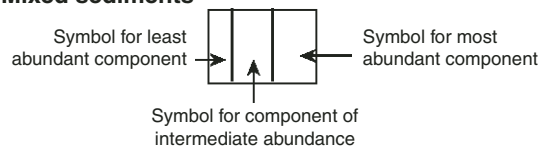


SB3

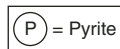
**Siliciclastic sediments**

















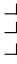


**Mixed sediments**



**Concretions**



**Figure F3.** Symbols used for drilling disturbance and sedimentary structure and bioturbation in the core descriptions (modified from Shipboard Scientific Party, 1995).

<b>Structure symbols</b>		<b>Drilling deformation symbols</b>	
—	Sharp contact		Thick color bands (sharp contact)
---	Gradational contact		Thick color bands (gradual contact)
◆	Isolated mud clast		Medium color bands (sharp contact)
◇	Isolated pebbles/cobbles		Medium color bands (gradual contact)
}	Slight bioturbation		Thin color bands (sharp contact)
}}	Moderate bioturbation		Thin color bands (gradual contact)
}}}	Heavy bioturbation		Laminations (millimeter scale)
			Concretions/nodules
			Pyrite nodule/concretion/burrows
			<b>Soft sediments</b>
			Slightly disturbed
			Moderately disturbed
			Very disturbed
			Drilling slurry or flow-in
			<b>Hard sediments</b>
			Slightly fractured
			Moderately fractured
			Highly fractured
			Drilling breccia



**Figure F4.** Compositional classification for siliciclastic marine sediments (modified from Myhre et al., 1995). The boundary between sandy silt and silty mud lies at 10%, as do other internal boundary lines.

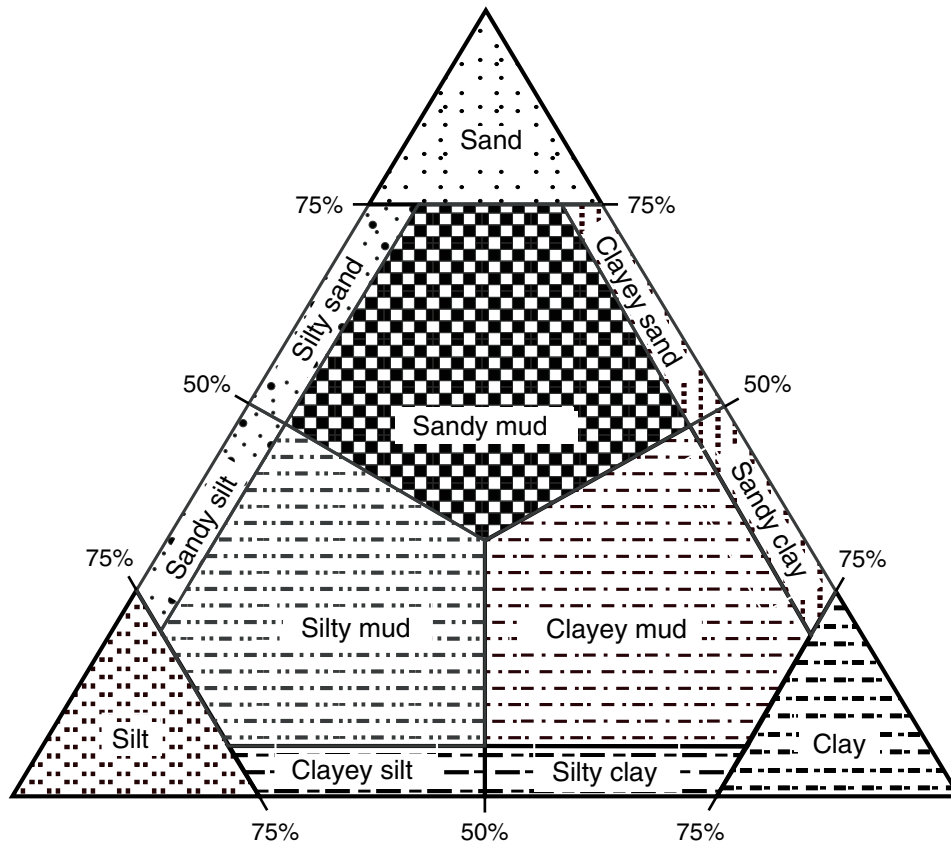


**Figure F5.** Compositional classification for biogenic and siliciclastic marine sediments. Mud (a mixture of sand, silt, and clay) is used as an example of the terrigenous component in this classification scheme (modified from Shipboard Scientific Party, 1995).

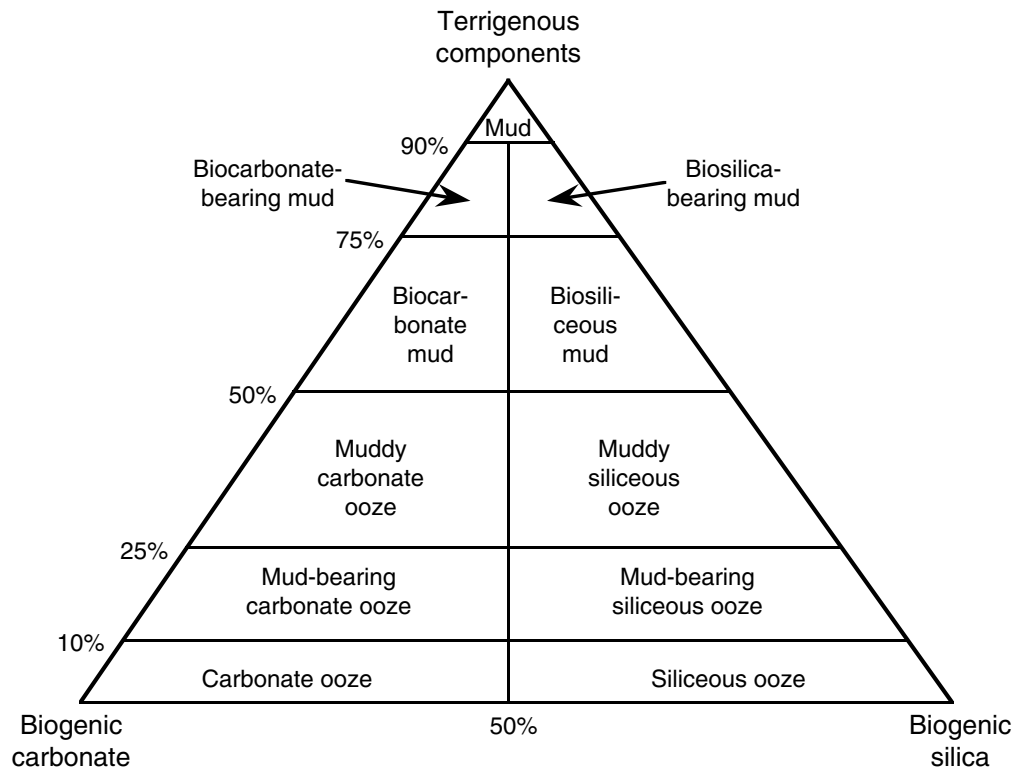


**Figure F6.** A. Selected interval of MS data from Holes 1218A, 1218B, and 1218C shown on the mbsf depth scale. Data from Holes 1218B and 1218C are offset by a constant for clarity. B. The same records are shown after depth-scale adjustment so that correlative features are aligned. C. The resulting spliced record is shown utilizing cores from Holes 1218A and 1218B.

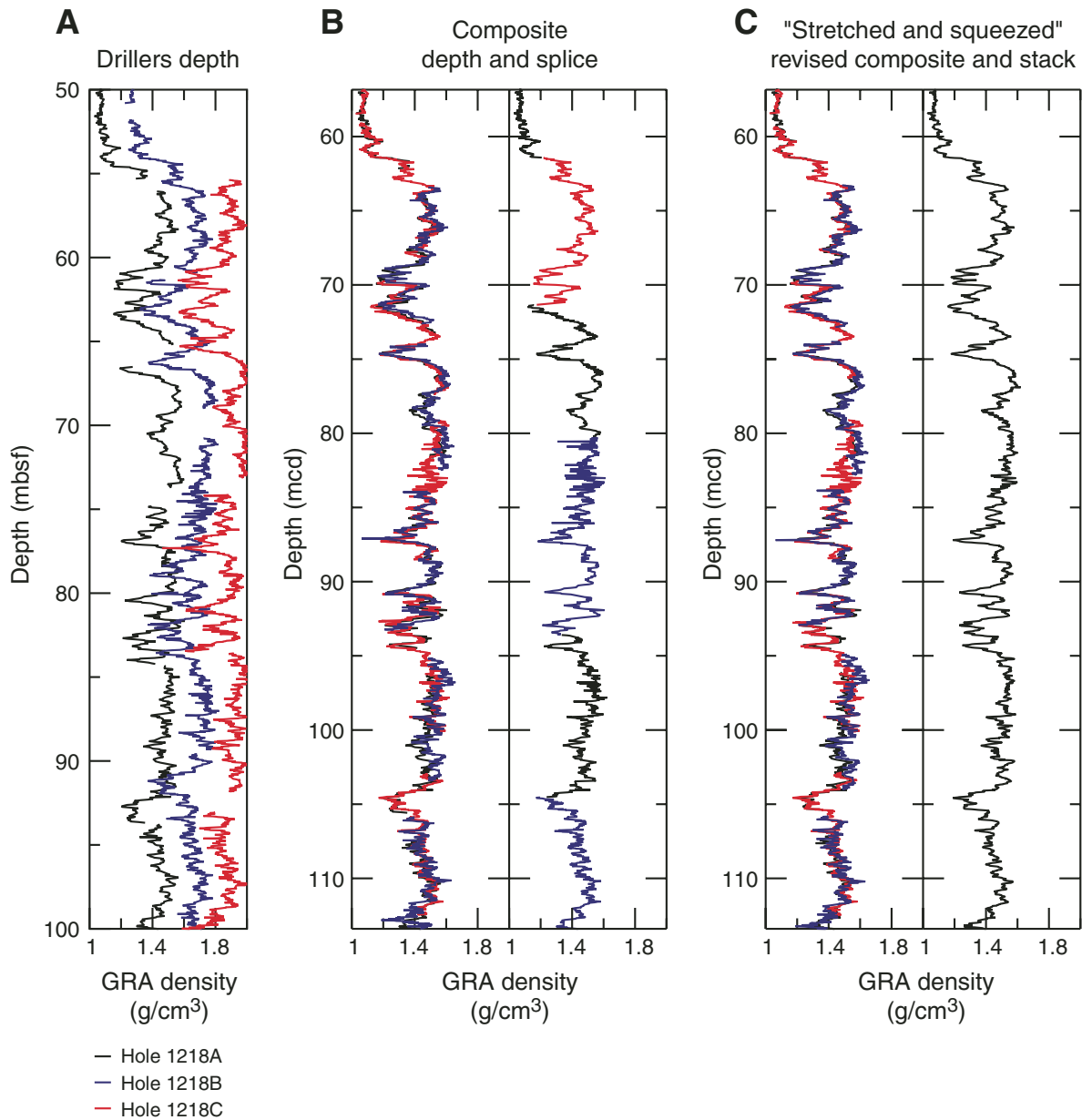


**Figure F7.** Illustration of the downhole logging tool string used during Expedition 302. SGT = Scintillation Gamma Ray Tool, NGT = Natural Gamma Ray Spectrometry Tool, BHC = Borehole Compensated Sonic Tool, GPIT = General Purpose Inclinometer Tool, and FMS = Formation MicroScanner.

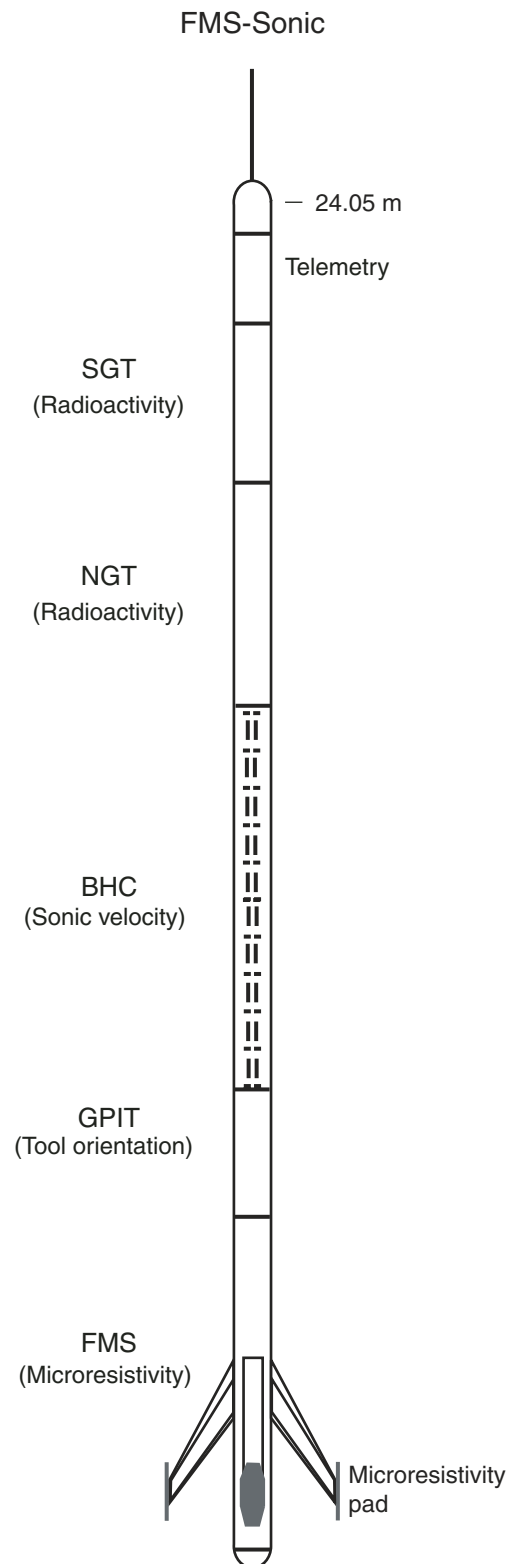




**Figure F8.** Photograph of high-pressure squeezers used during Expedition 302. Foreground: dismantled into individual components; background: collection of interstitial water.



**Figure F9.** Photographs of Rhizone samplers used during Expedition 302. A. Close-up of Rhizone sampler. B. Sampling interstitial waters from interval 302-M0002A-1X-1, 80–91 cm.

**A**



**B**

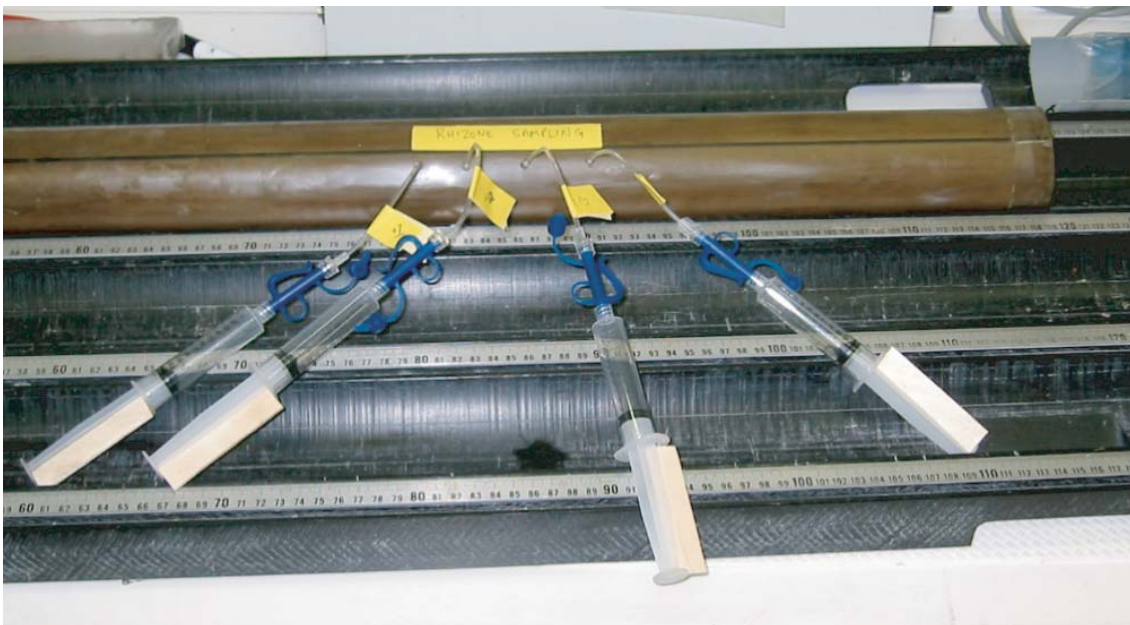
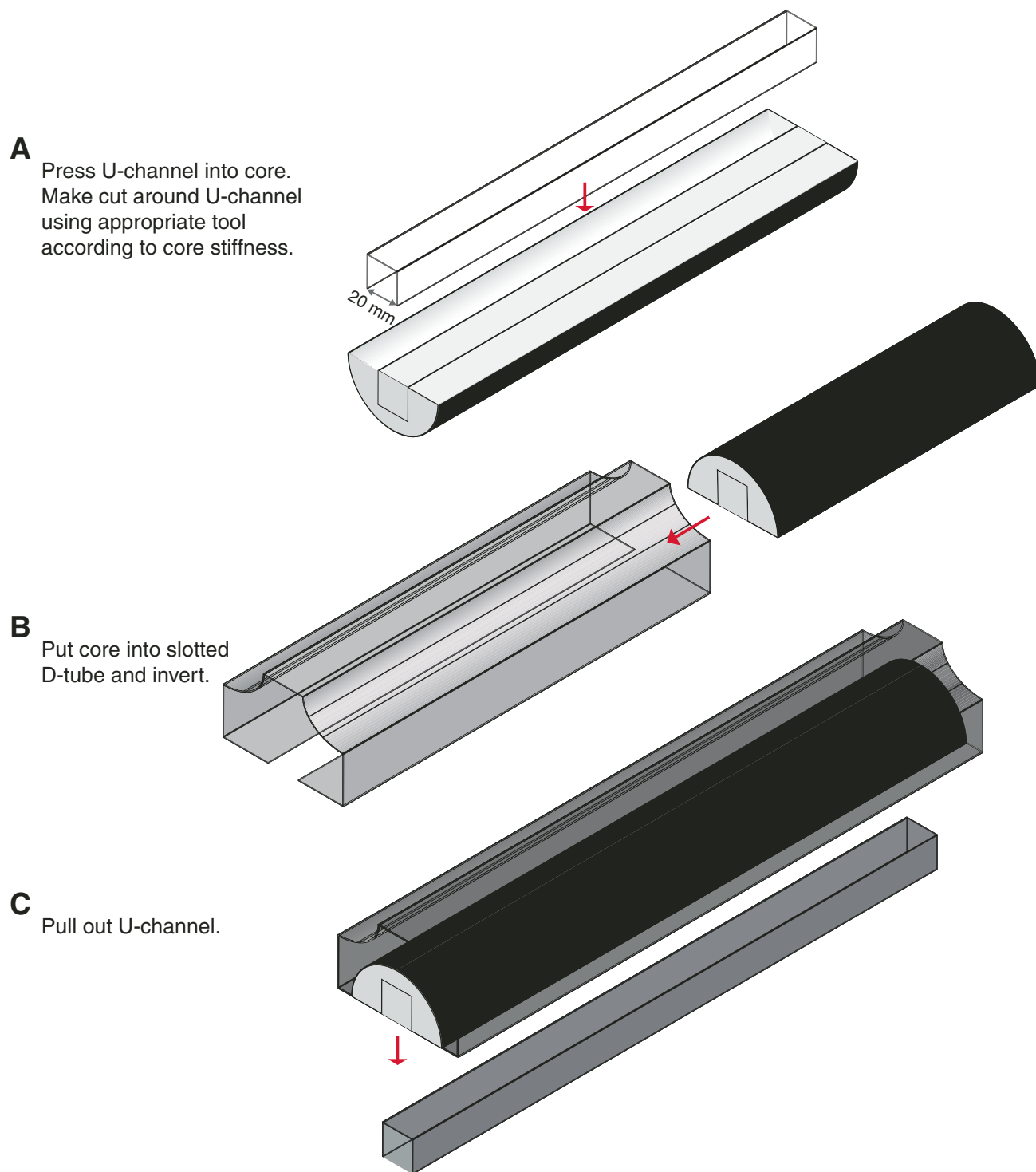


Figure F10. Schematic showing the method followed for sampling and extracting U-channel samples.



**Table T1.** Label identifiers for core types used.

Core type	Label identifier
Bit sample	B
Advanced piston corer (APC)	H
Miscellaneous	M
Rotary core barrel (RCB)	R
Wash core sample	W
Extended core barrel (XCB)	X
Advanced diamond core barrel (ADCB)	Z

**Table T2.** Example of disturbance table.

Core, section, interval (cm)	Quality
302-M0002A-	
3X-1, 0–8	Slurry
3X-1, 90–150	Slurry
3X-2	Slurry
3X-3	Slurry
3X-4	Flow-in
4X-1	Slurry
4X-2	Slurry
4X-3, 0–20	Slurry
4X-3, 20–150	Flow-in
4X-4, 0–30	Flow-in

Notes: Qualitative assessment ranges from good > slightly disturbed > disturbed > slurry biscuits > slurry. Flow-in = very distinct disturbance.



Table T3. Example of core vertical offset table (affine table), Site M0004.

Core	Offset (m)	Adjusted
302-M0004A-		
1H	-1.38	Y
2X	-1.38	N
3X	-1.38	N
4X	-3.9	Y
5X	-8.24	Y
6X	-8.54	Y
7X	-8.54	N
8X	-8.54	N
9X	-8.54	N
10X	-8.54	N
11X	-8.54	N
15X	-8.54	N
18X	-8.54	N
19X	-8.54	N
20X	-8.54	N
21X	-8.54	N
22X	-8.54	N
23X	-8.54	N
27X	-8.54	N
28X	-8.54	N
29X	-7.5	Y
30X	-8.54	N
31X	-8.54	N
32X	-8.54	N
33X	-8.54	N
34X	-8.54	N
35X	-8.54	N
41X	-8.54	N
42X	-8.54	N
302-M0004B-		
1X	5.91	Y
2X	0	N
3X	-2.01	Y
302-M0004C-		
1H	0	N
2H	-0.52	Y
3H	0	N
4H	0	N
5X	0	N
6X	-3.15	Y
8X	-3.15	N
9X	-3.15	N

Note: N = no, Y = yes.

Table T4. Example of splice table.

Hole, core, section, interval (cm)	Depth			Hole, core, section, interval (cm)	Depth	
	(mbsf)	(mcd)			(mbsf)	(mcd)
302-				302-		
M0004C-1H-1, 0	0.00	0.00		M0004C-2H-1, 26	4.26	3.74
M0004C-1H-4, 2	3.74	3.74	Tie to	M0003X-1H-3, 110	4.12	7.96
M0004C-2H-3, 146	8.48	7.96	Tie to	M0004C-3H-1, 0	8.95	8.95
M0003A-1H-4, 60	5.04	8.88	Append to	M0003X-2H-2, 42	6.92	12.99
M0004C-3H-3, 101	12.99	12.99	Tie to	M0004C-4H-1, 57	14.54	14.54
M0003A-2H-3, 46	8.47	14.54	Tie to	M0003X-3H-2, 42	11.92	17.71
M0004C-4H-3, 71	17.71	17.71	Tie to	M0002Z-5X-1, 45	16.96	19.73
M0003A-3H-3, 93	13.94	19.73	Tie to	M0002Z-6X-1, 63	22.13	21.51
M0002A-5X-2, 73	18.74	21.51	Tie to	M0002Z-7X-1, 0	26.50	25.88
M0002A-6X-4, 63	26.50	25.88	Append to			

Note: Site numbers were adjusted to be the same, with dummy hole letters, for import of different sites into Splicer.

**Table T5.** Measurements made by the wireline tool strings.

Tool string	Tool	Measurement	Sampling interval (cm)	Approximate vertical resolution (cm)
Formation MicroScanner (FMS)-sonic combination	FMS	Microresistivity	0.25	0.5
	GPIT	Tool orientation	0.25 and 15	NA
	NGT/SGT	Spectral gamma ray/total gamma ray	15	46/NA
	BHC	Acoustic velocity	15	61

Notes: All tool and tool string names are trademarks of Schlumberger. For the complete list of acronyms used in IODP and for additional information about tool physics and use consult IODP Logging Services at [iodp.ldeo.columbia.edu/TOOLS\\_LABS/](http://iodp.ldeo.columbia.edu/TOOLS_LABS/).

**Table T6.** Acronyms and units used for wireline logging tools.

Tool	Output	Tool name/Explanation of output	Unit
BHC		Borehole Compensated Sonic tool	
	DT	Compressional wave delay time ( $\Delta t$ )	ms/ft
FMS		Formation MicroScanner	
	C1, C2	Orthogonal hole diameters	inch
	P1AZ	Pad 1 azimuth	Degrees
		Spatially oriented resistivity images of borehole wall	
GPIT		General Purpose Inclinerometer Tool	
	DEVI	Hole deviation	Degrees
	HAZI	Hole azimuth	Degrees
	$F_x, F_y, F_z$	Earth's magnetic field (three orthogonal components)	Degrees
	$A_x, A_y, A_z$	Acceleration (three orthogonal components)	$m/s^2$
NGT		Natural Gamma Ray Spectrometry Tool	
	SGR	Standard total gamma ray	gAPI
	CGR	Computed gamma ray (SGR minus uranium contribution)	gAPI
	POTA	Potassium	wt%
	THOR	Thorium	ppm
	URAN	Uranium	ppm
SGT		Scintillation Gamma Ray Tool	
	ECGR	Environmentally corrected gamma ray	gAPI

Notes: All tool and tool string names are trademarks of Schlumberger. For the complete list of acronyms used in IODP and for additional information about tool physics and use consult IODP Logging Services at [iodp.ldeo.columbia.edu/TOOLS\\_LABS/](http://iodp.ldeo.columbia.edu/TOOLS_LABS/).

Table T7. Elemental contents of standards analyzed by XRF.

Element	MAG-1 (ppm)	Standard deviation (%)	Reported (ppm)	MAX (ppm)	Standard deviation (%)	CAMAX (ppm)	Standard deviation (%)
Al	83,400	1.0	86,800	89,000	0.7	90,600	0.9
As	7	18.8	9.2	28	6.8	4	10.4
Ba	490	12.1	480	320	12.8	400	8.1
Br	200	1.0	250	121	0.8	101	1.9
Ca	9,220	1.6	9,790	20,500	1.4	38,900	1.8
Cl	18,303	0.4	31,000	14,500	0.7	14,900	0.3
Co	51	17.0	20	54	4.3	80	15.9
Cr	95	22.0	97	106	17.7	66	31.8
Cu	26	12.0	30	29	15.5	47	13.8
Fe	45,600	0.5	47,600	66,800	0.5	43,400	0.1
Ga	21	9.2	20	20	10.5	21	19.1
K	27,700	1.1	29,500	12,800	1.4	12,800	1.7
Mg	19,900	3.3	18,000	13,300	2.7	15,600	0.3
Mn	740	3.0	760	210	16.1	1,380	2.8
Ni	46	10.0	53	53	10.6	74	2.5
P	830	6.2	699	760	2.7	470	24.5
Pb	31	7.2	24	27	6.5	28	4.1
Rb	127	1.8	150	69	3.7	72	2.7
S	3,120	1.3	3,900	7,950	1.1	4,400	1.1
Si	239,000	0.9	235,000	194,000	0.6	214,000	0.3
Sr	120	1.7	150	129	1.0	218	1.1
Th	18	17.0	12	15	18.6	21	4.9
Ti	3,900	3.2	4,500	4,000	1.4	4,500	6.9
V	130	20.0	140	270	8.7	178	27.3
Zn	119	3.3	130	109	4.3	118	4.5

Notes: MAG-1 = U.S. Geological Survey marine sediment standard;  $N = 16$ . MAX = University of Bremen internal standard;  $N = 6$ . CAMAX = University of Bremen internal standard;  $N = 3$ . XRF = X-ray fluorescence.